

ACTIVE VIBRATION CONTROL OF A SMART PLATE

A DISSERTATION

*Submitted in partial fulfilment of the
requirements for the award of the degree*

of

MASTER OF TECHNOLOGY

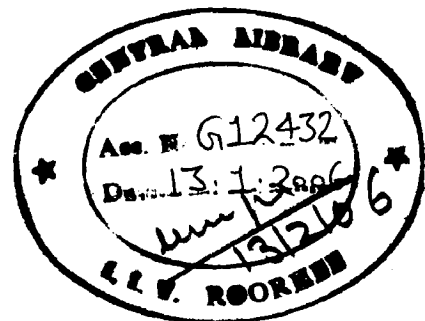
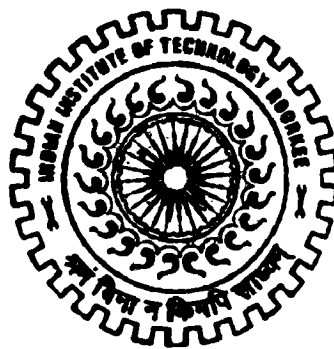
In

MECHANICAL ENGINEERING

(With Specialization in Machine Design Engineering)

By

ANANT S. PATIL



DEPARTMENT OF MECHANICAL AND INDUSTRIAL ENGINEERING
INDIAN INSTITUTE OF TECHNOLOGY ROORKEE
ROORKEE-247 667 (INDIA)

JUNE, 2005

CANDIDATE'S DECLARATION

I hereby declare that work is being presented in the dissertation entitled “**ACTIVE VIBRATION CONTROL OF A SMART PLATE**” towards partial fulfillment of the requirements for the award of the degree of **Master of Technology in Mechanical Engineering** with specialization in **Machine Design Engineering**, submitted to the Department of Mechanical and Industrial Engineering, Indian Institute of Technology, Roorkee, is an authentic record of my own work carried out from July 2004 to May 2005, under the guidance of **Prof. S.C. Jain**, Department of Mechanical and Industrial Engineering, I.I.T. Roorkee.

I have not submitted the matter embodied in this dissertation for the award of any other degree or diploma.

Date: 29-06-2005

Place: Roorkee



(ANANT PATIL)

CERTIFICATE

This is to certify that the above statement made by the candidate is correct to the best of my knowledge.

Date: 29-06-2005

Place: Roorkee


(**Prof. S.C. JAIN**)
Department of Mech. & Ind. Engg.
I.I.T. Roorkee
Roorkee- 247667
INDIA

ACKNOWLEDGEMENT

“Obstacles are those frightful things you see when you take off your goal”

And with no exception, this was the condition when I started this work. But in the due course of time with the thorough guidance of my project guide, it has come to a success. Though the deepest gratitude can only be felt inside heart, but in words, with my deepest esteem I thank my beloved teacher, **Prof. S.C.Jain**, my guide, for his continued guidance, enthusiastic help and numerous valuable suggestions during the thesis work.

I am very grateful to Prof. V.K.Goel, Head of the department of mechanical and industrial engineering, who supported my effort.

I express my gratitude to all the teachers of the department who had been source of inspiration to me and also to Mr. Rajeev Kumar, Research scholar, for his guidance.

I also would like to thank all my friends and the non teaching staff of the department who have directly or indirectly contributed in understanding the subject and constantly encouraged while carrying out this work.

- ANANT PATIL

ABSTRACT

Active vibration control and using piezoelectric sensors and actuators have recently emerged as a practical and promising technology. Efficient and accurate modeling of these structures bonded to or embedded with actuators and sensors is needed for efficient design of smart structures. This dissertation addresses the modeling of these structures and the associated control system design technique.

For piezoelectric laminates the governing equations of motion are derived using First Order Shear Deformation Theory (FSDT) and the dynamic response fields inside the laminate are obtained. A finite element approach for design of a structure and its control system for suppressing vibration is presented. A finite element model for a smart plate with surface bonded piezoelectric patches is developed using a quadratic rectangular element. Genetic algorithms are used to approximate the optimum locations of the piezoelectric actuators over a plate. The objective function for the genetic algorithm is taken as the energy dissipated by the controller. The modal analysis is carried out to establish the dynamic characteristics of the system before and after the application of actuators.

CONTENTS

Candidate's Declaration	I
Acknowledgement	II
Abstract	III
Contents	IV
Nomenclature	VIII
List of Figures	X
List of Tables	XI
Chapter 1 INTRODUCTION	1
1.1 Motivation	1
1.2 Preamble	2
1.3 Organization of the thesis	3
Chapter 2 BACKGROUND	5
2.1 Active control strategies in vibration suppression	5
2.2 Perspective in smart structures	6
2.3 Piezoelectric materials	8
2.3.1 Piezoelectric effect	9
2.3.2 Piezoelectric materials	10
2.3.3 Classification of piezoelectrics	10
2.3.4 Piezoelectric materials in vibration control	10
2.4 Optimal actuator placement over the plate	10
Chapter 3 LITERATURE REVIEW	13
Chapter 4 THEORETICAL MODELING	24
4.1 First order shear deformation theory	24
4.2 Boundary conditions	26
4.3 Finite Element Model	27
4.4 Energy equations	29

4.5	First order shear deformation theory	33
4.6	Location optimization of actuators	40
Chapter 5	GENETIC ALGORITHMS	43
5.1	Description	43
5.2	Fundamentals	45
5.3	What are GAs?	45
5.4	Basic steps in genetic algorithm	47
5.4.1	Encoding scheme	47
5.4.2	Fitness function	48
5.4.3	Parent selection	48
5.4.4	Crossover	49
5.4.5	Mutation	50
5.4.6	Replacement strategies	51
5.4.7	Convergence criterion	51
5.4.8	Performance criterion	52
Chapter 6	RESULTS AND DISCUSSION	53
6.1	Boundary Conditions	54
6.2	Static analysis results	56
6.2.1	Effect of Grid size on max deflection of the plate.	56
6.2.2	The effect of fiber orientation in an orthotropic material on maximum static deflection.	58
6.2.3	Effect of h/L on maximum deflection for a cross ply laminated plate which is simply supported.	60
6.3	Dynamic analysis results:	62
6.3.1	Dynamic Analysis of isotropic plate	62
6.3.2	Dynamic Analysis of orthotropic plate	63
6.3.3	Variation of Natural frequencies with the orientation angle for a cantilevered plate	68
6.3.4	Variation of the fundamental natural frequencies with patch coverage area	70
6.4	Actuator placement optimization	72

	6.5 Time response	75
Chapter 7	CONCLUSION AND SCOPE FOR FUTURE WORK	76
	7.1 Conclusion	76
	7.2 Scope for Future Work	76
	REFERENCES	77

LIST OF FIGURES

Figure 2.1: A closed loop control system	5
Figure 2.2: Classification of Piezoelectric Materials	10
Figure 4.1: Deformed and undeformed geometries of an edge of a plate under the assumption of CPT	24
Figure 4.2: Deformed and undeformed geometries of an edge of a plate under the assumption of FSDT	24
figure 4.3: Boundary conditions for simply supported and clamped edges under the assumptions of FSDT	25
Figure 4.4 :Four noded rectangular element	26
Figure 5.1 Typical genetic algorithm	46
Figure 5.2: Roulette wheel	48
Figure 5.3: Crossover	49
Figure 5.4: Mutation	50
Figure 6.1: Degrees of freedom at each node	53
Figure 6.2: Boundary conditions for a simply supported plate	54
Figure 6.3: Boundary conditions for a cantilever plate	54
Figure 6.4: Boundary conditions for a clamped plate	55
Figure 6.5: Maximum deflection obtained for different grid sizes for a simply supported plate	57
Figure 6.6: Maximum deflection obtained for different grid sizes for a cantilevered plate	57
Figure 6.7: Maximum deflection obtained for different grid sizes for a clamped plate	58
Figure 6.8: Variation of Max deflection with the orientation angle: Simply supported plate	59
Figure 6.9: Variation of Max deflection with the orientation angle Cantilever plate	60
Figure 6.10: Variation of Max deflection with the thickness of plate Simply supported plate	61

Figure 6.11: 1st Mode shape: Simply supported orthotropic plate	65
Figure 6.12: 2nd Mode shape: Simply supported orthotropic plate	65
Figure 6.13: 1st Mode shape: Clamped orthotropic plate	66
Figure 6.14: 2nd Mode shape: Clamped orthotropic plate	66
Figure 6.15: 1st Mode shape: Cantilevered orthotropic plate	67
Figure 6.16: 2nd Mode shape: cantilevered orthotropic plate	67
Figure 6.17: The variation of first natural frequency with orientation angle for a cantilevered orthotropic plate	68
Figure 6.18: The variation of second natural frequency with orientation angle for a cantilevered orthotropic plate	69
Figure 6.19: The variation of natural frequency with piezoelectric patch coverage area for a cantilevered orthotropic plate.	71
Figure 6.20: Plate surface showing 100 elements	72
Figure 6.21: Optimized location of actuators over the cantilevered plate	73
Figure 6.22: Actuator locations when only the first mode is considered	74
Figure 6.23: Actuator locations when only the second mode is considered	74
Figure 6.24: Time response of the system before and after the application of force	75

LIST OF TABLES

Table 6.1: Deflections for different grid sizes for plate with different boundary conditions.	56
Table 6.2: Deflections for different orientation angle of the fibers for a simply supported and cantilevered plate	59
Table 6.3: Deflections for different thickness to side length ratios for a simply supported plate using different grid sizes.	61
Table 6.4: Natural frequencies for an isotropic simply supported plate	62
Table 6.5: Natural frequencies for an isotropic clamped plate	62
Table 6.6: Natural frequencies for an isotropic cantilever plate	63
Table 6.7: Natural frequencies for an orthotropic simply supported plate	64
Table 6.8: Natural frequencies for an orthotropic clamped plate	64
Table 6.9: Natural frequencies for an orthotropic cantilever plate	64
Table 6.10: First natural frequencies for a cantilevered plate for different orientation angles	68
Table 6.11: Second natural frequencies for a cantilevered plate for different orientation angles	69
Table 6.12: Natural frequencies for a cantilevered plate for different coverage area of the piezoelectric patch	70
Table 6.13: The best 12 individuals obtained by GA.	73

NOMENCLATURE

ABBREVIATIONS

AVC	Active Vibration Control
DOF	Degrees of Freedom
ER	Electro-Rheological
FBC	Feedback Control
FEM	Finite Element Method
FFC	Feed Forward Control
FOS	Fiber Optic Sensor
FSMA	Ferromagnetic Shape Memory Alloys
HVC	Hybrid Vibration Control
IMSC	Independent Modal Space Control
LQR	Linear Quadratic Gaussian
MIMSC	Modified Independent Modal Space Control
MR	Magneto-Rheological
MSM	Magnetic Shape Memory Alloys
PVC	Passive Vibration Control
PVDF	Polyvinylidene Fluoride
PZT	Lead Zirconate Titanate
MD Sensor	Modal Domain Optical Fiber Sensor
DQ	Differential Quadrature
SMA	Shape Memory Alloys
CPT	Classical Plate Theory
FSDT	First Order Shear Deformation Theory
GA	Genetic algorithm
SGA	Simple Genetic algorithm
BC	Boundary condition

SYMBOLS

\bar{x}, y, z	Global coordinates
u, v, w	Displacement at node along x,y,z direction respectively
u_0, v_0, w_0	Displacement of mid plane at a node along x,y,z direction respectively
m, n	Direction cosines
θ	Orientation angle of fibers
$[Q]$	Elastic coefficient matrix
N_i	Shape functions
q	Displacement vector
ϵ	Strain component
γ	Shear strains
σ	Axial stress
τ	Shear stress
$\partial/\partial x$	Differential operator with respect to x
E	Young's modulus, Electric field
ν	Poisson's ratio
G	Shear modulus
V	Strain Energy
T	Kinetic energy
W	Work done
$[M]$	Mass matrix
$[K]$	Stiffness matrix
$[C]$	Damping matrix
ξ	Damping coefficient
$\{F\}$	Force vector
E	Electric field
G	Gain
ω	Natural frequency
ρ	Density of the material
$[\phi]$	Modal matrix
p	Number of actuators
n	Number of modes
t	time, thickness

PI	Performance index
λ	Eigen value
A	Area of Cross-Section
{F}	Stress Resultant
{M}	Bending Stress Resultant
{S}	Transverse shear force Resultant

SUPERCRIPTS

A	Actuator
S	Sensor
T	Transpose
-1	Inverse

Chapter 1. INTRODUCTION

1.1 Motivation:

All the mechanical systems are subjected to various conditions that may result in vibrational motion; hence vibration is a significant factor to be considered in the design of lighter mechanical systems, systems working at high speeds and the systems like micro sensing, micro actuation, space structures etc. where accuracy finds a great importance. Vibrations may lead to fatigue in the material, damage to the structure, deterioration of system performance, increased noise level and increase in the difficulty of predicting the behavior of the structure. Active vibration methods can be used to eliminate the undesired vibrations. The use of smart structures is experiencing a tremendous growth in actively controlling the vibration.

Advanced composite materials are finding increasing application in aircraft, automobiles, marine and submarine vehicles besides other engineering applications. The fiber-reinforced composites possess two desirable features: one is their high stiffness-weight ratio and the other is their anisotropic material property that can be tailored through variation of the fiber orientation and stacking sequence- a feature which gives the designer an added degree of flexibility. In this paper a finite element model for a composite plate has been developed using the first order shear deformation theory for laminated plates to analyze the behavior of piezoelectric material over a plate structure.

The field of smart structures has been an emerging area of research for the last few decades. Smart structures or intelligent structures can be defined as structures that are capable of sensing and actuating in a controlled manner in response to an input. The ability of the piezoelectric materials to convert electrical to mechanical energy and vice versa makes them to be employed as actuators and sensors. If these are bonded properly on to a structure, structural deformations can be induced by applying a voltage to the materials, employing them as actuators. Similarly, these piezoelectric materials can also be employed as sensors since deformations of a structure would cause the deformed

piezoelectric materials to produce an electric charge. The extent of structural deformation can be observed by measuring the electrical voltage the sensors produce. This voltage is multiplied by some gain according to the control law implemented and is fed back to the actuators. The actuators made of smart materials react to the voltage and generate mechanical changes. Using the changes from the actuators, the vibration or other dynamic characteristics can be closely controlled.

For a complex structure, it is very expensive to implement smart materials over the entire surface. Hence the sensors and actuators are usually discretely distributed over the structure. One of the limitations of piezoelectric actuator is the amount of the force it can exert. Hence it is important that the actuators are placed at optimal locations so that the required control effort is minimum. Thus optimization of placement of these sensors and actuators over the structure becomes an important task in suppressing the vibration of the structure. The problem becomes critical as the number of sensors/actuators to be used over the structure increases and as the mode shape becomes complicated. Therefore optimization techniques have to be used in such cases to find a good set of sensors/actuator positions. The significance in using such algorithms is not only the solution to problems but also, drastically cost savings in both experimental and time expenses. Genetic algorithm produces a global optimum and can be applied to complicated problems with relative ease. It is more flexible and provides more accurate solution.

This work deals with the modeling of a composite plate using finite element method assuming the first order shear deformation theory for plates. The dynamic characteristics of the structure are studied and piezoelectric patches are used to control its vibration. The optimum locations of the piezoelectric actuators are approximated using genetic algorithm. The objective function for the genetic algorithm is taken as the energy dissipated by the controller. The modal analysis is carried out to establish the dynamic characteristics of the system before and after the application of actuators.

1.2 Preamble

The primary objectives of this study are to develop a simple finite element for multilayered composite plates. The element contains five degrees of freedom, three displacements and two slopes. (i.e. shear rotations) per node. The accuracy of the element is demonstrated through the problems. Our objective is to study the dynamic characteristics of the structure before and application of the piezoelectric patches over the plate. Further the implementation of genetic algorithm to optimize the location of the actuators over the plate structure, taking the objective function as the minimization of the energy dissipated by the controller and finally to obtain the dynamic response of the structure using the modal analysis before and after the application of the piezoelectric actuators over the plate.

1.3 Organization of the thesis:

Chapter 2 addresses some theoretical background needed for the work. The strategies in the active vibration control have been discussed. Some perspectives in smart structures and piezoelectric materials have been given. It also introduces genetic algorithms and discusses their advantages.

Chapter 3 contains a brief discussion regarding the previous work that has been done in this field. Summarized details of work carried out by different authors, their objectives and conclusions are given.

Chapter 4 details the development of the finite element model using the first order deformation theory, the derivation of the equations is given in detail along with the development of the objective function for genetic algorithms to optimize the location of the actuator/sensors.

Chapter 5 discusses the optimization of the actuators over the plate. The use of genetic algorithms is discussed. The objective function is derived in this section which is then used in the algorithm for optimizing.

Chapter 6 shows the solution to various problems considered. The results are discussed with the help of graphs and figures.

Chapter 2. BACKGROUND

This chapter covers the explanation regarding the active control strategies for the vibration suppression, the smart structures which includes a brief description of the piezoelectricity and lastly the genetic algorithms are explained in detail.

2.1 Active control strategies for vibration suppression

A control system is considered to be any system that exists for the purpose of regulating or controlling the flow of energy, information, money, or other quantities in some desired fashion. A control system is an interconnection of many components or functional units in such a way as to produce a desired result. In a closed loop or active control system, there is typically some model of the system to be controlled, a control law, and some sensors that make measurements to carry out the control. Figure 2.1 shows a block diagram of a typical closed loop control system. In this control system, the control $U(t)$ is modified by information obtained about the system output, $Y(t)$.

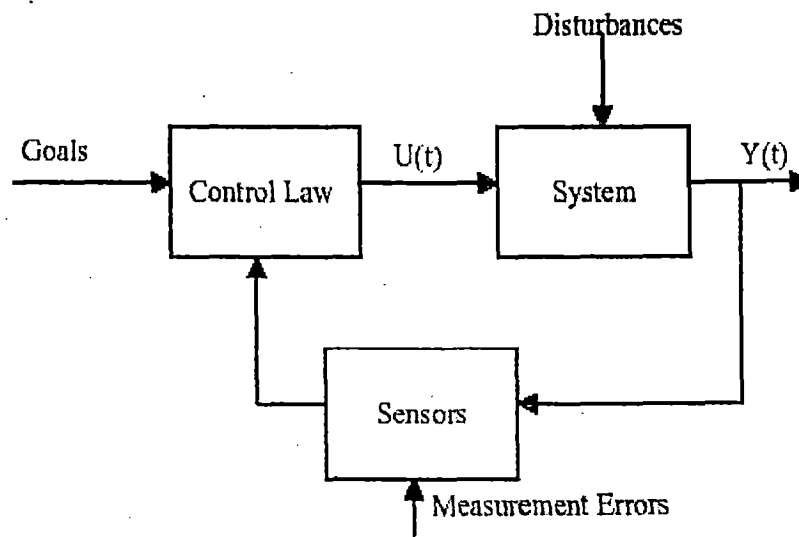


Figure 2.1: A closed loop control system

The feedback closed loop control system shown in Figure 2.1 represents a typical continuous control system.

2.2 Perspectives in Smart Structures.

The field of smart structures has been an emerging area of research for the last few decades. Smart structures (also called smart material structures) can be defined as structures that are capable of sensing and actuating in a controlled manner in response to a stimulus. The development of this field is supported by the development in the field of materials science and in the field of control. In materials science, new smart materials are developed that allow them to be used for sensing and actuation in an efficient and controlled manner. These smart materials are to be integrated with the structures so they can be employed as actuators and sensors effectively. It is also clear that the field of smart structures also involves the design and implementation of the control systems on the structures. A well designed and implemented controller for smart structures is thus desirable.

In this thesis, we consider the case of vibration of smart structures. The stimulus to a structure may originate from external disturbances or excitations that cause structural vibrations. A smart structure would be able to sense the vibration and generate a controlled actuation to itself so the vibration can be minimized. For vibration control purposes, a number of smart materials can be used as actuators and sensors such as piezoelectric, shape memory, electrostrictive and magnetostrictive materials. Here, we concentrate on using piezoelectric materials because they have good broadband sensing and actuation properties.

Different smart materials include:

- **Shape Memory Alloy (SMA):** The term Shape Memory Alloys (SMA) is applied to a group of metallic materials that can return to a previously defined shape when subjected to an appropriate thermal procedure. Generally, these materials can be plastically deformed at some relatively low temperature, and upon exposure to some higher temperature will return to their shape prior to the deformation. SMAs allow one to recover up to 5% strain from the phase change induced by temperature. SMAs

are best suited for one-way tasks such as deployment. SMAs are little used in vibration control. Examples are Ni-Ti alloys, Cu-Zn-Al, Cu-Al-Ni, Fe-Mn, and Fe-Mn-Si, etc.

- **Piezoelectric Materials:** Piezoelectricity is the ability of a material to develop an electrical charge when subjected to a mechanical strain and conversely. They have a recoverable strain of 0.1% under electric field; they can be used as actuators as well as sensors. Examples are PZT, PVDF, etc.
- **Magnetostrictive Materials:** As a magnetostrictive material is magnetized, there is a change in length. Conversely if an external force produces a strain in magnetostrictive materials, its magnetic state will change. Magnetostrictive materials have a recoverable strain of 0.15% under magnetic field; the maximum response is obtained when the material is subjected to compressive loads. They can be used in high precision applications. Example is Terfenol-D.
- **Electrostrictors (Electrostrictive Materials):** These are quite similar to piezoelectric materials with slightly better strain capability, but very sensitive to temperature. The conceptual difference between piezoceramics and electrostrictors is their response upon reversing of the electric field. Piezoceramics can be elongated and compressed, while electrostrictors only exhibit an elongation, independent of the direction of the applied electric field. This effect is found in all materials, though in very small quantities 10^{-5} to 10^{-7} %.
- **Ferromagnetic Shape Memory Alloy (FSMA):** Ferromagnetic shape memory alloys (FSMA) are a recently discovered class of actuator materials, whose salient features are magnetically driven actuation and large strains (around 6%) e.g. NiMn-Ga ternary alloy. As the name suggests FSMA's are ferromagnetic alloys that also support the shape memory effect.

- **Electro-Rheological (Er) And Magneto- Rheological (MR) Fluids:** When an external electric field is applied to an ER fluid, the viscosity of the fluid increases remarkably. And when the electric field is taken away, the viscosity of the fluid goes back to the original state. The phenomenon is so called ER effect. These fluids can change from a thick fluid (similar to motor oil) to nearly a solid substance within a span of a millisecond when exposed to an electric field; the effect can be completely reversed just as quickly when the field is removed. MR fluids experience a viscosity change when exposed to magnetic field. Examples of MR fluid is tiny iron particles suspended in oil and that of ER fluid are milk chocolate or cornstarch and oil.
- **Fiber Optics:** Fiber optics is becoming popular as sensors because they can be easily embedded in composite structures with little effect on the structural integrity. They are widely used in Structural Health Monitoring equipments.

2.3 Piezoelectric Materials

In 1880, Pierre and Paul-Jacques Curie discovered the direct piezoelectric effect on various crystals such as tourmaline, Rouchelle salt and quartz. The crystals generated electrical charges on their surfaces when they were mechanically strained in certain directions. In the following year, they also discovered the converse piezoelectric effect that the shape of crystals would change when an electric field was applied to them.

The ability of the piezoelectric materials to exchange electrical and mechanical energy opens up the possibility of employing them as actuators and sensors. If the piezoelectric materials are bonded properly to a structure, structural deformations can be induced by applying a voltage to the materials, employing them as actuators. On the other hand, they can be employed as sensors since deformations of a structure would cause the deformed piezoelectric materials to produce an electric charge. The extent of structural deformation can be observed by measuring the electrical voltage the materials produce. Unfortunately, the piezoelectric effect in natural crystals is rather weak so they cannot be used effectively as actuators or sensors.

However, recent developments in the field of materials science have provided piezoelectric materials that have sufficient coupling between electrical and mechanical domains. Two of the commonly used piezoelectric materials are polyvinylidene fluoride (PVDF), a semi crystalline polymer film, and lead zirconate titanate (PZT), a piezoelectric ceramic material. PZT has larger electromechanical coupling coefficients than PVDF so PZT can induce larger forces or moments on structures. However, PZT is relatively brittle while PVDF is flexible and can be easily cut into any desired shape. PVDF also has good sensing properties so it is commonly used for sensors. In this thesis, we concentrate on using PZT as actuators and sensors. Our results show that PZT can be effectively used as a transducer for vibration control of flexible structures.

2.3.1 Piezoelectric Effect

The piezoelectric effect was first discovered in 1880 when Pierre and Currie demonstrated that certain crystalline material produces an electrical charge on its surface when it is subject to a stress field. It was subsequently demonstrated that the converse effect is also true; when an electric field is applied to the piezoelectric material, its shape and size change. In the former case, the material works like a sensor while in the latter case, the material can be used as an actuator if it is constrained against deformation.

2.3.2 Piezoelectric Materials

They are two broad classes of piezoelectric materials used in vibration control: ceramics and polymers. The piezopolymers are used mostly as sensors; because they require high voltages as well as they are lightweight and flexible so they are not effective as actuators on stiff structures. The best known is the polyvinylidene fluoride (PVDF) (PVF₂). Piezoceramics are used extensively as actuators and sensors, for a wide range of frequency including ultrasonic applications. The best-known piezoceramic is Lead Zirconate Titanate (PZT) [Pb (Zr, Ti) O₃].

Piezoelectric materials offer a number of advantages over conventional actuators like low energy consumption, fast response, high efficiency and compactness. But they have some limitations also like voltage that can be applied is limited in the range of -500 V to 1500 V, the piezo materials cannot be used above their curie temperature, which is 200°C to 300 °c due to possibility of depolarization.

2.3.3 Classification Of Piezoelectrics

Pyroelectrics: materials in which electric field generates as a result of application of heat and degree of polarization depends on the temperature.

Ferroelectrics: materials in which spontaneous polarization can be induced by an electric field. Reversing external electric field can change their polarization direction. Examples are PZT and PVDF.

Ferro elastics: materials in which spontaneous polarization can be induced due to mechanical load.

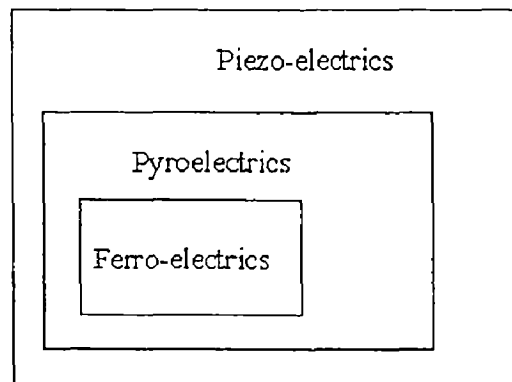


Figure 2.2 Classification of Piezoelectric Materials

2.3.4 Piezoelectric Materials In Vibration Control

Coupled electro-mechanical properties of piezoelectric ceramics and polymers and their availability in thin sheets make them well suited for the use as sensors and actuators. Piezoelectric materials are widely used in vibration control due to their competitive performance. Besides these, the lightweight actuators don't affect significantly the mass and stiffness properties of the original structure, so the original

dynamic characteristics of the structure remain unchanged when the piezoelectric patches are not activated.

Piezoelectric patches apply two types of effects on structures:

Passive - Change in mass and stiffness characteristics (this effect is negligible for stiff structures), and

Active - Generation of charge and strain due to applied stress and voltage respectively.

Resonance is said to occur when the excitation frequency matches any of the natural frequencies of the system, so one should know the natural frequencies of the system, hence the eigenvalues of plate with and without patches have been calculated. The contribution of patches in mass and stiffness matrices has been considered. The piezoelectric patches location over the plate is also optimized using the genetic algorithm so as to obtain an optimal control of vibrations of the plate.

2.4 Optimal Placement Of Actuators/Sensors Over The Plate

Optimal placement of actuators is finding a great importance in the field of research in these days. One of the limitations of a piezoelectric material is the amount of force it can exert. Hence, it is important to optimize the locations of the actuators so that the required control effort is minimum. Similarly, to obtain a good signal to noise ratio, sensors should be chosen to provide maximum output for the vibration in the modes of interest. These problems become more critical as the number of actuators and sensors increases and the mode shapes become more complicated. Sometimes we find that the structure has close (or exactly the same) frequencies. For the same reasons, it necessary to use multiple actuators and sensors. As the mode shapes become more complicated the modal interactions of actuators and sensors are also quite complicated. Therefore, it necessitates use optimization techniques to find a good set of actuators and sensors. Out of several optimization techniques, we choose a genetic algorithm (GA), in this thesis as it can produce a global optimum solution and can be applied to complicated problems with relative ease to optimize the location of actuators over the plate. The detailed explanation of the genetic algorithm is given in chapter 5.

The next chapter discusses about the previous work that is carried by different authors in the field of vibration control using the smart materials. It includes the brief introduction of their work done and conclusions derived by them.

Chapter 3. LITERATURE REVIEW

Smart structures, incorporating piezoelectric materials, offer an efficient method for implementing active control technologies and as a consequence the topic has received considerable interest in recent years. Piezoelectric materials have been widely used for sensors and actuators due to their attractive properties, such as low weight and rapid response. Below, some relevant work in the area of vibration control using the smart structures is reviewed.

Crawley and de Luis [1987] developed analytical models to predict the static and dynamic response of intelligent systems to an applied voltage. These models were applicable to systems with segmented piezoelectric actuators that are either bonded to an elastic member or embedded in a laminated composite structure. They also consider perfect bonding conditions between the actuators and the structure as well as bonds of finite thickness and stiffness. The models were used to select an optimal location for actuators. With a PZT consisting of two piezoceramic actuator devices bonded at equal but opposite distances from the neutral axis of the beam, three experimental systems were constructed: an aluminum beam with two surface-mounted PZTs, a glass-epoxy beam with two PZTs and a graphite-epoxy beam with one PZT. The PZTs were used to excite steady-state resonant vibrations in the beams and the experimental responses were seen to agree with the analytical models. Static tests performed on the glass-epoxy laminated material with embedded PZTs showed a reduction in ultimate strength of only 20% and no significant change in the global elastic modulus of the composite laminate.

In the work from which his Master of Science thesis arose, Collins et al. [1990] provided a brief but informative history of piezoelectricity and some of the basic physical properties and mathematical relationships used in the study of piezoelectric materials. The fact that other noncrystalline materials, such as wood, bone and some polymers, exhibit piezoelectric behavior is discussed. In particular, the discovery of the

piezoelectric effect in polyvinylidene fluoride (PVDF) is presented. In its unpolarized form, PVDF is a clear, lightweight and tough yet highly flexible film that is often used as a passive protective coating for many surfaces due to its high resistance to various chemicals and ultraviolet light. After suitable processing consisting of stretching at high temperatures, exposure to high electric fields during cooling (poling) and surface metallization, PVDF can be used as a sensor and/or actuator for active structural control. After the outstanding introduction to the history, manufacturing and application of piezopolymers, Collins et al. proceeds to model and experimentally verify the use of PVDF as modal sensors and spatial filters for various mechanical systems.

Hagood, Chung and von Flotow [1990] presented a more detailed consideration of the interaction between an elastic structure and piezoelectric actuators used for active structural control. Also, they developed state space models for voltage and current-driven piezoelectric devices and assessed how the dynamics of the actuator and passive electrical network influence the overall system dynamics. These models are used to predict the behavior of a cantilevered beam with surface-mounted piezoceramic devices. Lastly, open- and closed-loop control experiments were performed to verify the analytical models, thus showing significant effects of the electrical circuit on the beam dynamics.

Cox and Lindner [1991] discussed in their paper, the use of a modal domain optical fiber sensor (MD Sensor) as a component in an active control system to suppress vibrations in a flexible beam. An MD Sensor consists of a laser source, an optical fiber, and detection electronics. They have shown that the output of the MD Sensor is proportional to the integral of the axial strain along the optical fiber.

Kulkarni and Hanagud [1991] developed an electromechanical model for a combined generic three-dimensional, isotropic, linearly elastic body and piezoelectric body undergoing small or large deformations using a variational formulation. The model is

then used to develop a two-dimensional finite element formulation to predict the static and dynamic response of the system to applied voltages that vary with time and spatial distribution on the surface of the patch. A detailed treatment of the electromechanical coupling between the active element and the elastic body is presented. The stresses and strains predicted by the static analytical model were verified using a cantilevered aluminum beam with piezoceramic patches bonded to the top and the bottom surfaces. The same beam was used to verify the dynamic response of the system to various types of applied voltages. It was found that electric fields applied to the actuators in a non-uniform manner, such as a linear, cosine or exponential variation along its length, result in different types of bending moment distributions being applied to the beam.

Hinton E. et. al., 1995, dealt with the free vibration analysis of prismatic folded plate and shell structures supported on diaphragms at two opposite edges with the other two edges arbitrarily restrained. The analysis was carried out by using curved\ variable thickness finite strips based on Mindlin_Reissner shell theory, which allows for transverse shear deformation and rotatory inertia effects. The accuracy and relative performance of a family of C0 strips were examined. Results are presented for a series of problems including plates, cylindrical shells and box girders. In a companion paper these accurate and inexpensive finite strips were used for structural shape optimization.

Banks, Smith and Wang [1995] examined the interaction between piezoelectric actuators on such structures as beams, plates and more complicated shell structures such as a right circular cylinder. The changes in mechanical stiffness of the structure due to the attachments were studied in addition to the ability of the patches to apply forces and moments, which were found to depend on the geometry and placement of the patch in addition to the applied voltage. The influence of internal forces and moments due to the structure and the actuator as well as those due to actuating the patch are then related to the time-dependent structural equations of motion. With that, these models can be applied directly to controlling the vibration of such structures, particularly those of a

curved nature. Since the structure at the focus of this research was a toroidal shell, the results from Banks, Smith and Wang will contribute greatly when control of the entire inflated member is considered.

Langley [1995] claimed in his paper that the equations for natural frequencies developed by Rayleigh are invalid. Since the point mobility of a membrane has an infinite imaginary component, any inertial force created by an attached point mass would lead to an infinite displacement at that point. Clearly this is not the case; however, it was found that large deformations do take place around the attachment that can only be represented by a multi-term Rayleigh-Ritz method. With this approach, Langley presents solutions for the free vibration of a circular membrane with a point mass attachment as well as the forced response of a square membrane with a point mass attachment using the modal summation method. The results are used to understand the physical limitations of linear membrane theory with point mass attachments. In order to obtain more accurate results, he suggests the use of a nonlinear theory, considering the attachment to have a finite area or taking into account the finite bending stiffness of the membrane (i.e., plate theory).

Niekerk and Tongue [1995] investigated ways to actively reduce the transient noise transmission through a membrane covering a circular duct. Once the nature of the sound has been identified, only a few milliseconds are available to determine the control signal and actuate the structure. Therefore, piezopolymer actuators were used because they offer the ability to operate at high frequencies. Their experiment used a speaker to impart sound waves into a duct whose cross-section is covered by an elastic membrane fitted with discrete piezopolymer (PVDF) actuators. The sound pressure imparted to the film was measured immediately before the membrane by a microphone. The resulting velocity of the center of the membrane was measured with a laser vibrometer, whose output was used as a feedback signal for the control loop. The output of this control loop was given to the PVDF actuators attached to the membrane. The resulting sound pressure level was measured at a microphone on the side of the membrane opposite the

speaker. Three control schemes were investigated analytically, and then experimentally, namely optimal control, sliding control and velocity feedback control. It was found that a reduction in transient noise transmission through the membrane was possible. Experimental results confirmed this analytical prediction. The PVDF actuators performed fast enough to control the membrane and velocity feedback was found to be the most stable and easily implemented control method.

Suleman and Venkayya, (1995), developed finite element formulations for composite plates with laminated piezoelectric layers. They developed 24 degrees of freedom piezoelectric plate elements with one electrical degree of freedom per surface. They made assumptions that the electrical degrees of freedom were constant along the plane and vary linearly through the thickness of the piezoelectric layers. An advantage of their methodology is that the analysis eliminates problems associated with modeling thin plate elements with isoparametric solid elements, which have excessive shear strain energies and higher stiffness in the thickness directions.

Masad [1996] studied a rectangular membrane with uniform tension and thickness, but with linearly varying density along one dimension of the membrane. Solutions to natural frequencies and mode shapes were obtained using both a numerically accurate analytical technique and approximation methods for the inhomogeneous membrane. The resulting frequencies and mode shapes were compared to those of an equivalent, homogeneous membrane. As expected, some variation was seen between the two types of membranes and the approximate method was able to closely predict the natural frequencies.

A square membrane under uniform tension with a centrally located circular area of finite radius and either continuously or discontinuously varying density was considered by Bambill, et al. [1997]. He determines the natural frequencies using both the Optimized Rayleigh-Ritz method and an approximate conformal mapping approach. Reasonable agreement is seen between the two methods for the discontinuously varying density.

Likewise, acceptable results are obtained for the square membrane with circular center section of continually varying density.

Saravanos, D.A. (1997), developed finite elements that enable the formal analysis of piezoelectric composite shells. His methodology was based on what is called a "Mixed Laminate Theory." This theory utilizes unique approximations for displacements and electric potentials. The first order shear deformation theory was assumed on the mechanical displacements, while discrete layer ("layer wise") approximations are assumed on the electrical potentials. The advantages of this mixed laminate theory are they

- 1.) Accurately and efficiently model thin and/or moderately thick laminated piezoelectric shells with arbitrary laminations and electric configurations, and they
- 2.) Captured the through-the-thickness electric heterogeneity induced by the embedded piezoelectric layers.

Finite element methods were compared to exact solutions. The analysis was justified with excellent convergence and agreement with fundamental frequencies and through-the-thickness electromechanical modes of moderately thin plates.

Jinsong *et al.* [1998] used a FOS and ER fluid actuator for vibration monitoring of smart composite structures. They found same sensitivity in FOS as piezoelectric materials with lower cost. They found change in structural damping and natural frequencies with varying electric field and hence vibrations can be monitored by using FOS and ER fluid.

Of particular interest to the present study, Pronsato *et. al.* [1999] considers a rectangular membrane under uniform tension with a rectangular center section having a constant density different than the rest of the structure. Again, approximation techniques are used to find the frequency coefficients, from which natural frequencies can be extracted. The approximation was made possible by using a truncated Fourier series consisting of a linear combination of sine waves to approximate the displaced shape of the vibrating

membrane. The results are tabulated for different ratios of density between the outer and inner areas as well as different dimensions of the inner rectangular section. Finally, good correlation is seen when the results are compared to a previous paper in which only one polynomial expression was used to represent the displacement of the membrane. It can be shown that results attained by Pronsato are even more accurate than those of the previous paper.

Payman Afshari and G. E. O. Widera, (2000), developed a series of plate elements, based on the modified complementary energy principal, to study the free undamped vibration response of laminated composite plates. They selected Mindlin thin plate theory to govern the general characteristics and behavior of these plate elements. A series of in-plane strain functions were assumed from which the corresponding in-plane strains and corresponding stresses for each lamina were determined. The transverse stresses were then computed by satisfying the equations of the equilibrium. Eight-noded isoparametric elements were utilized to describe the displacement field. These hybrid plate elements are used to form the stiffness and the consistent mass matrices. The fundamental natural frequencies were then computed by solving the generalized eigenvalue problem and their application demonstrated via a number of examples.

Wang and Chen (2000) performed a modal analysis of a simply supported plate using only PZT patches as actuators and PVDF patches as sensors. Their work included a theoretical development of the interaction between the smart actuators and sensors with the steel plate, generation of a column in the frequency response function matrix, generation of the plate's mode shapes, and extraction of the plate's modal parameters. They acknowledged that smart materials have a major advantage over the conventional structural testing. Piezoceramic transducers can be integrated into the structure, and that the idea of using smart materials for system identification is also important to other applications such as structural vibration and acoustic control.

Sze and Yao [2000] prepared a number of finite element models for modelling of smart structures with segmented piezoelectric patches. These included eight-node solid shell element for modelling homogeneous and laminated host structures as well as an eight-node solid shell and a four-node piezoelectric membrane element for modelling surface bonded piezoelectric sensing and actuating patches. They studied number of problems with these models and found results agreeing with experimental results.

Clayton L. Smith, (2001), demonstrated that multiple layer modeling is achievable by single layer equivalent modeling using equivalent material properties. He derived finite element methods for modeling piezoelectric structures, which account for mechanical and electrical characteristics of the structure and validated the linear theory of piezoelectricity with ABAQUS models using piezoelectric elements. He also demonstrated equivalent single layer techniques for modeling piezoelectric laminated structures and determined equivalent loading techniques for modeling piezoelectric structures and piezoelectric laminated structures subject to electrical loading conditions. He simplified the analysis of piezoelectric laminated structures such that computational models can be developed to investigate the static and dynamic response using equivalent representations of the structure.

Makhecha D.P. et. al.,(2002), studied the effects of higher-order theory, that accounts for the realistic variation of in-plane and transverse displacements through the thickness, on the modal loss factors and natural frequencies of thick composite laminated/sandwich plates. They presented a displacement-based C0 continuous isoparametric, eight-noded quadrilateral plate element, based on realistic higher-order theory. The accuracy and effectiveness of the present model over the first- and other higher-order theories for vibration and damping characteristics were demonstrated considering thick laminated/sandwich plates. They suggested that, the higher-order terms such as stretching term in the transverse displacement field, slope discontinuity in thickness direction for in-plane displacements, and various other high order terms are important in

evaluating the damping and forced response characteristics of sandwich laminates. This mainly depends on the ply-angle, lamination scheme, aspect ratio and core thickness.

Yan Y.J. and Yam L.H., 2002, presented in their paper the optimal design methodology of number and locations of actuators in active vibration control of a space truss using multiple piezoelectric ceramic stack actuators. They applied eigenvalue distribution of the energy correlative matrix of the control input force, to determine the optimal number of actuators required, and genetic algorithms (GAs) were adopted to search for the optimal locations of actuators. Their results showed that the disturbance acting on a structure is a key factor in determining the optimal number and locations of actuators in active structural vibration control, and a global and efficient optimization solution of multiple actuator locations can be obtained using the GAs.

Liew K.M. et. al., (2003) , suggested that in conventional analyses of composite laminates, the assumption of perfect bonding of adjoining layers is well accepted, although this is an oversimplification of the reality. It is possible that the bond strength may be less than that of the laminate. Thus, the study of weak bonding is an interesting focus area. In their study, an elastic bonding model based on three-dimensional theory of elasticity in a layer wise framework is used to study composite laminates. The differential quadrature (DQ) discretization is used to analyze the layer wise model. The present model enables the simulation of actual bonding stress states in laminated structures. The interfacial characteristics of transverse stress continuity as well as the kinematics continuity conditions were satisfied through the inclusion of the elastic bonding layer. Their model was employed to investigate the free vibration of thick rectangular cross-ply laminates of different boundary conditions and lamination schemes.

Peng F et.al.(2003) investigated the actuator placement on a plate structure and vibration control of the structure. They optimized the location of actuators based on maximizing

the controllability grammian. It was implemented using structuring analysis in ANSYS and genetic algorithm. Further they used a filtered-x LMS based multichannel adaptive control to suppress the vibrations. They also performed the numerical simulations in suppressing tri sinusoidal response at three points of the plate. Their results demonstrated that the genetic algorithm is an effective method to reduce the energy required for achieving significant vibration reduction.

Shimpi R.P. and Ainapure, (2004), extended, variationally consistent layer-wise trigonometric shear deformation theory to deal with free vibration of two-layered laminated cross-ply plates. They Derived Governing differential equations by making use of a displacement field which allows a sinusoidal variation of the in-plane displacements through the laminate thickness. And concluded that, in their displacement based theory, constitutive relations between shear-stress and shear-strains are satisfied in both the layers, and, therefore, shear correction factor is not required. Compatibility at the layer interface in respect of in-plane displacement and compatibility in respect of transverse shear-stress is satisfied, yet present theory contains fewer unknown variables than that of the first order shear deformation theory. Effects of rotary inertia and other inertias are also included. They also suggested that their theory will be convenient for finite element modeling and finite element based on the present theory will be free from shear locking. From the illustrative example, it is seen that the present theory gives the accurate results. Efficiency of the theory was demonstrated through illustrative examples.

Chapter 4. THEORETICAL MODELLING

In this chapter we develop the equations relevant to the problem. First the first order deformation theory for laminated plates is introduced. Then a laminated composite plate is considered to derive its stiffness and mass matrices using the finite element method under the assumptions of the first order shear deformation theory. Further the governing equations for static and dynamic analysis of the plate are derived. Then the modal analysis for the plate along with the piezoelectric patches is discussed along with the equations. The objective function for the genetic algorithm is then derived by minimizing dissipation of the energy.

4.1 First Order Shear Deformation Theory:

Classical plate theory is based on the assumptions that a straight line perpendicular to the plane of the plate is (1) inextensible, (2) remains straight, and (3) rotates such that it remains perpendicular to the tangent to the deformed surface. i.e. the transverse normal and shear stresses are neglected. Thus it underpredicts the deflections and over predicts the frequencies as well as buckling loads of plates. That is why it is necessary to use some other theory. [Reddy. J.N, 2003]

The first order shear deformation theory (FSDT) extends the kinematics of the classical plate theory by relaxing the normality restriction and allowing for arbitrary but constant rotation of transverse normals [Reddy. J.N, 1998]. It means the condition (3) is removed. The more significant difference between the CPT and FSDT is the effect including the shear deflections on the predicted deflections, frequencies and buckling loads. So the primary objective in developing analytical solution for the rectangular plates using FSDT is to bring out the effects of shear deformations on deflection, stresses, frequencies and buckling loads.

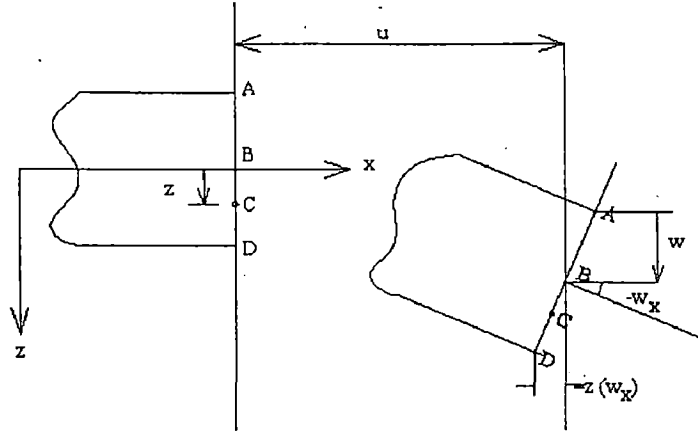


Figure 4.1: Deformed and undeformed geometries of an edge of a plate under the assumptions of CPT

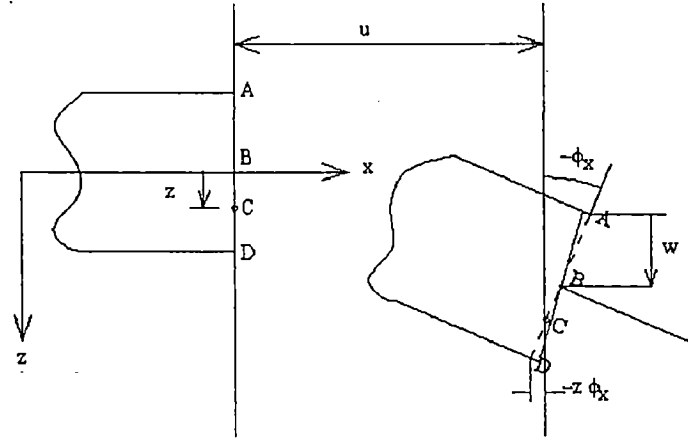


Figure 4.2: Deformed and undeformed geometries of an edge of a plate under the assumptions of FSDT

The linear constitutive elastic field equation for a typical layer is given by

$$\begin{Bmatrix} \sigma_x \\ \sigma_y \\ \tau_{xy} \end{Bmatrix}_k = \begin{bmatrix} m^2 & n^2 & -2mn \\ n^2 & m^2 & 2mn \\ mn & -mn & m^2 - n^2 \end{bmatrix}^T \begin{bmatrix} Q_{11} & Q_{12} & Q_{16} \\ Q_{12} & Q_{22} & Q_{26} \\ Q_{16} & Q_{26} & Q_{66} \end{bmatrix}_k \begin{bmatrix} m^2 & n^2 & -2mn \\ n^2 & m^2 & 2mn \\ mn & -mn & m^2 - n^2 \end{bmatrix} \begin{Bmatrix} \varepsilon_x \\ \varepsilon_y \\ \gamma_{xy} \end{Bmatrix}_k$$

$$\begin{Bmatrix} \tau_{yz} \\ \tau_{xz} \end{Bmatrix}_k = \begin{bmatrix} m & n \\ -n & m \end{bmatrix}^T \begin{bmatrix} Q_{44} & Q_{45} \\ Q_{45} & Q_{55} \end{bmatrix}_k \begin{bmatrix} m & n \\ -n & m \end{bmatrix} \begin{Bmatrix} \gamma_{yz} \\ \gamma_{xz} \end{Bmatrix}_k \quad (4.1)$$

where

$m = \cos\theta$, $n = \sin\theta$, θ is skew angle and Q_{ij} are the elastic stiffness coefficients,

A doubly curved shell is taken with coordinates x, y along the in plane direction and z along the thickness direction. Based on FSDT of small strains, the displacement u, v, w at a point (x, y, z) and independent rotation θ_x and θ_y of Normal in xz and yz planes respectively as:

$$\begin{aligned} u(x, y, z, t) &= u_o(x, y, t) + z\theta_x(x, y, t) \\ v(x, y, z, t) &= v_o(x, y, t) + z\theta_y(x, y, t) \\ w(x, y, z, t) &= w_o(x, y, t) \end{aligned} \quad (4.2)$$

Where

u, v and w are the displacement components in the piezoelectric composite plate space along x, y and z axes respectively,

u_o, v_o and w_o are displacements of the reference point (x, y) on the midplane ($z=0$)

θ_x and θ_y are the slopes of the normal to the reference point (x, y) on the midplane in yz and xz planes respectively.

4.2 Boundary conditions:

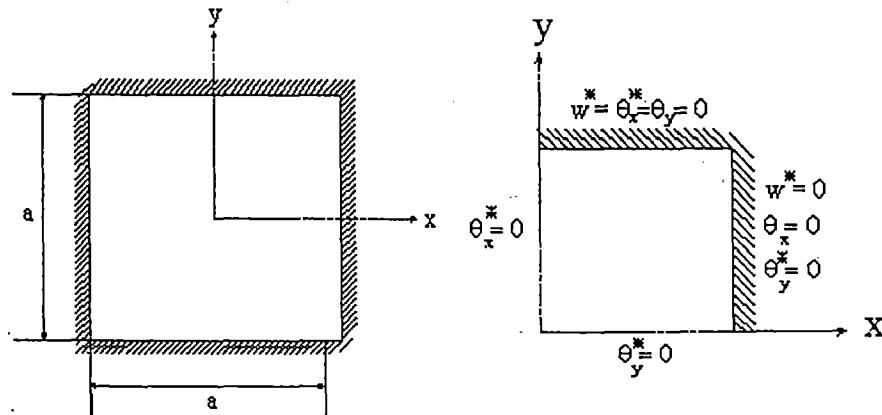


Figure 4.3: Boundary conditions for simply supported (quantities with an asterisk only) and clamped edges.

Figure 4.3 shows various types of boundary conditions on an edge of the plate element for the first order shear deformation theory. When the edge is parallel to the x or y axis, the normal and tangential components of a variable become the y and x (or x and y) components, respectively, of the variable [Reddy J.N.,2003].

4.3 FEM Formulation:

A simple 4 noded rectangular element is considered.

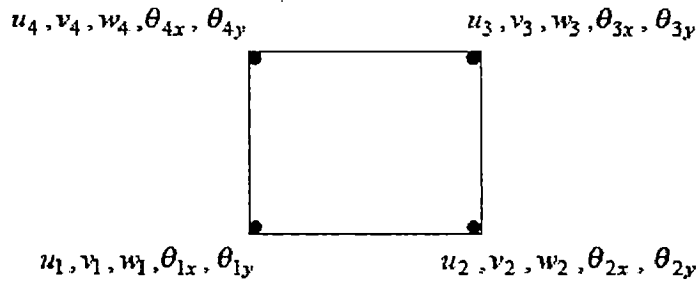


Figure 4.4: Four noded rectangular element

Displacement functions: Two dimensional interpolation (shape) functions are used to define the geometry field at any point in the element cross-section. These shape function relate the curvilinear coordinates in the nodal Cartesian coordinate system to the element coordinate system

$$\begin{aligned}
 N_1 &= \frac{1}{4}(1-\xi)(1-\eta) & N_2 &= \frac{1}{4}(1+\xi)(1-\eta) \\
 N_3 &= \frac{1}{4}(1+\xi)(1+\eta) & N_4 &= \frac{1}{4}(1-\xi)(1+\eta)
 \end{aligned} \tag{4.3}$$

The element has five elastic degree of freedom u_o, v_o, w, θ_x and θ_y per node,

$$\{q_i\}_e = [u_{o_i} \quad v_{o_i} \quad w_i \quad \theta_{x_i} \quad \theta_{y_i}]^T \quad i=1,2,3,4$$

Each variable of the degree freedom can be represented n terms of the shape function as

$$u_o = [N_{u_o}] \{q\} \quad v_o = [N_{v_o}] \{q\} \quad w = [N_w] \{q\} \quad \theta_x = [N_{\theta_x}] \{q\} \quad \theta_y = [N_{\theta_y}] \{q\} \tag{4.4}$$

And the displacement field within the element can be given as:

$$\bar{u} = \begin{Bmatrix} u \\ v \\ w \\ \theta_x \\ \theta_y \end{Bmatrix} = [N_u] \{q\} = \sum_{i=1}^4 N_i [I]_{5 \times 5} \begin{Bmatrix} u_{o_i} \\ v_{o_i} \\ w \\ \theta_{x_i} \\ \theta_{y_i} \end{Bmatrix} \quad (4.5)$$

Assuming small deflection and considering the effect of shear deformation. The total strain can be expressed as:

$$\{\varepsilon\} = \begin{Bmatrix} \varepsilon_p \\ 0 \end{Bmatrix} + \begin{Bmatrix} z\varepsilon_b \\ \varepsilon_s \end{Bmatrix} \quad (4.6)$$

Where the midplane (membrane) strain $\{\varepsilon_p\}$, bending strain $\{\varepsilon_b\}$ and shear strain $\{\varepsilon_s\}$ is given by

$$\{\varepsilon_p\} = \begin{Bmatrix} \frac{\partial u_o}{\partial x} \\ \frac{\partial v_o}{\partial y} \\ \frac{\partial u_o}{\partial y} + \frac{\partial v_o}{\partial x} \end{Bmatrix} = \sum_{i=1}^4 \begin{bmatrix} \frac{\partial N_{u_{o_i}}}{\partial x} & 0 & 0 & 0 & 0 \\ 0 & \frac{\partial N_{v_{o_i}}}{\partial y} & 0 & 0 & 0 \\ \frac{\partial N_{u_{o_i}}}{\partial y} & \frac{\partial N_{v_{o_i}}}{\partial x} & 0 & 0 & 0 \end{bmatrix} \begin{Bmatrix} u_{o_i} \\ v_{o_i} \\ w_i \\ \theta_{x_i} \\ \theta_{y_i} \end{Bmatrix} = [B_p] \{q\} \quad (4.7a)$$

$$\{\varepsilon_b\} = \begin{Bmatrix} \frac{\partial \theta_x}{\partial x} \\ \frac{\partial \theta_y}{\partial y} \\ \frac{\partial \theta_x}{\partial y} + \frac{\partial \theta_y}{\partial x} - \frac{\partial u_o}{\partial y} - \frac{\partial v_o}{\partial x} \end{Bmatrix} = \sum_{i=1}^4 \begin{bmatrix} 0 & 0 & 0 & \frac{\partial N_{\theta_{x_i}}}{\partial x} & 0 \\ 0 & 0 & 0 & 0 & \frac{\partial N_{\theta_{y_i}}}{\partial y} \\ \frac{\partial N_{u_{o_i}}}{\partial x} & \frac{\partial N_{v_{o_i}}}{\partial y} & 0 & \frac{\partial N_{\theta_{x_i}}}{\partial y} & \frac{\partial N_{\theta_{y_i}}}{\partial x} \end{bmatrix} \begin{Bmatrix} u_{o_i} \\ v_{o_i} \\ w_i \\ \theta_{x_i} \\ \theta_{y_i} \end{Bmatrix} = [B_b] \{q\} \quad (4.7b)$$

$$\{\varepsilon_s\} = \begin{Bmatrix} \theta_x - \frac{\partial w}{\partial x} \\ \theta_y - \frac{\partial w}{\partial y} \end{Bmatrix} = \sum_{i=1}^4 \begin{bmatrix} 0 & 0 & -\frac{\partial N_{w_i}}{\partial x} & N_{\theta_{x_i}} & 0 \\ 0 & 0 & -\frac{\partial N_{w_i}}{\partial y} & N_{\theta_{y_i}} & 0 \end{bmatrix} \begin{Bmatrix} u_{o_i} \\ v_{o_i} \\ w_i \\ \theta_{x_i} \\ \theta_{y_i} \end{Bmatrix} = [B_s] \{q\} \quad (4.7c)$$

4.4 Energy equations

Potential energy equation:

Using constitutive equation, the in-plane stress-strain behavior of the k th lamina of the laminate is represented as [Rajeev Kumar ,2003]

$$\begin{Bmatrix} \sigma_x \\ \sigma_y \\ \tau_{xy} \end{Bmatrix} = [\overline{Q}_{ij}] \left(\{\varepsilon_p\} + z \{\varepsilon_b\} \right) \quad (4.8)$$

Where $[\overline{Q}_{ij}] = [T_b]^T [Q] [T_b]$

If $\{F\}$ represents the membrane stress resultants (F_{xx}, F_{yy}, F_{xy}) and $\{M\}$ represents the bending stress resultants (M_{xx}, M_{yy}, M_{xy}) we can relate these to membrane strains $\{\varepsilon_p\}$ and the bending strains $\{^TM_b\}$, through the constitutive relations as:

$$\begin{aligned} \{F\} &= [A_{ij}] \{\varepsilon_p\} + [B_{ij}] \{\varepsilon_b\} \\ \{M\} &= [B_{ij}] \{\varepsilon_p\} + [D_{ij}] \{\varepsilon_b\} \end{aligned} \quad (4.9)$$

Where,

$$[A_{ij}] = \sum_{k=1}^n \int_{h_{k-1}}^{h_k} [\overline{Q}_{ij}] dz \quad [B_{ij}] = \sum_{k=1}^n \int_{h_{k-1}}^{h_k} [\overline{Q}_{ij}] z dz \quad [D_{ij}] = \sum_{k=1}^n \int_{h_{k-1}}^{h_k} [\overline{Q}_{ij}] z^2 dz \quad (4.10)$$

The transverse shear stress of the k th layer can be written as :

$$\begin{Bmatrix} \tau_{xz} \\ \tau_{yz} \end{Bmatrix}_k = [\overline{Q}_{ij}] \{\varepsilon_s\}_k \quad \text{Where } i, j = 4, 5 \quad (4.11)$$

It is assumed that shear stress is not influencing the piezoelectric effect.

If $\{S\}$ represent the transverse shear force resultant (S_{xz}, S_{yz}) , then it is related to the transverse shear strain through the constitutive relation:

$$\{S\} = [H_{ij}] \{\varepsilon_s\} \quad (4.12)$$

Where, $\{H_{ij}\} = \sum_{k=1}^n k_{\alpha i} k_{\alpha j} \int_{h_{k-1}}^{h_k} [\overline{Q}_{ij}]_k dz$

Where $k_{\alpha i}$, $k_{\alpha j}$ being shear correction factors as per reissner's variation method

$$k_{\alpha i} =, k_{\alpha j} = 5/6$$

Using the variation principle the strain energy functional, V is given by

$$V = \frac{1}{2} \left[\int_A \left(\{\varepsilon_p\}^T \{F\} + \{\varepsilon_b\}^T \{M\} + \int_A \{\varepsilon_s\}^T \{S\} \right) dA \right] \quad (4.13)$$

On putting value from equation (4.8) in to (4.10)

$$V = \frac{1}{2} \left[\int_A \left(\{\varepsilon_p\}^T [A_{ij}] \{\varepsilon_p\} + \{\varepsilon_p\}^T [B_{ij}] \{\varepsilon_b\} \right) dA \right] + \frac{1}{2} \left[\int_A \left(\{\varepsilon_b\}^T [B_{ij}] \{\varepsilon_p\} + \{\varepsilon_b\}^T [D_{ij}] \{\varepsilon_b\} \right) dA \right] + \frac{1}{2} \left[\int_A \left(\{\varepsilon_s\}^T [H_{ij}] \{\varepsilon_s\} \right) dA \right] \quad (4.14)$$

On putting values from equation (4.5) & (4.7) in above equation

$$V = \frac{1}{2} \left[\{q\}^T \int_A \left([B_p]^T [A_{ij}] [B_p] + [B_p]^T [B_{ij}] [B_b] + [B_b]^T [B_{ij}] [B_p] + [B_b]^T [D_{ij}] [B_b] + [B_s]^T [H_{ij}] [B_s] \right) dA \{q\} \right] \quad (4.15)$$

Say

$$[k] = \int_A \left([B_p]^T [A_{ij}] [B_p] + [B_p]^T [B_{ij}] [B_b] + [B_b]^T [B_{ij}] [B_p] + [B_b]^T [D_{ij}] [B_b] + [B_s]^T [H_{ij}] [B_s] \right) dA$$

On putting these values in above equation

$$V = \frac{1}{2} \{q\}^T [k] \{q\} \quad (4.16)$$

Kinetic energy equation:

The element kinetic energy is:

$$T = \frac{1}{2} \int_A \left(p \left(\dot{u}_o^2 + \dot{v}_o^2 + \dot{w}^2 \right) + I \left(\dot{\theta}_x^2 + \dot{\theta}_y^2 \right) \right) dA \quad (4.17)$$

Where

$$p = \sum_{k=1}^{n_l} \int_{h_{k-1}}^{h_k} \rho dz \quad I = \sum_{k=1}^{n_l} \int_{h_{k-1}}^{h_k} z^2 \rho dz$$

On putting displacement in terms of shape function

$$T = \frac{1}{2} \{q\}^T [m] \{q\} \quad (4.18)$$

Where

$$[m] = \int_A \left(p \left([N_{u_o}]^T [N_{u_o}] + [N_{v_o}]^T [N_{v_o}] + [N_w]^T [N_w] \right) + I \left([N_{\theta_x}]^T [N_{\theta_x}] + [N_{\theta_y}]^T [N_{\theta_y}] \right) \right) dA \quad (4.19)$$

Work done by the external forces and electrical charge:

The virtual work done by the surface force & the applied electrical charge density is given by:-

$$\delta W^s = \int_s \{\delta \bar{u}\}^T \{f_s\} ds \quad (4.20)$$

Where $\{f_s\}$ and $\{f_q\}$ are the surface force density and surface electrical charge density respectively. s_1 and s_2 the surface area where the surface forces and electrical charge are applied respectively.

On putting value of displacement & electrical field in above equation.

$$\delta W^s = \{\delta q\}^T \{F_s\} \quad (4.21)$$

Where

$$\{F_s\} = \int_{s_1} [N_u] \{f_s\} ds$$

The Langrangian L of a bonded piezoelectric body is defined by the summation of all kinetic energy & potential energy (included strain and electrical energies)

$$L = T - V + W^e \quad (4.22)$$

Hamilton's principle assumes that the energy variation over an arbitrary period of time is *Zero*, i.e.

$$\int_{t_0}^{t_f} \delta(L + W^s) dt = 0 \quad (4.23)$$

On putting value if L from equation (4.22)

$$\int (\delta T - \delta V + \delta W^s) dt = 0 \quad (4.24)$$

It is assumed that the dynamic coupling of heat transfer with structural deflection and electric field are small. The temperature field can be calculated based on the given thermal excitation using the principles of heat transfer.

Different terms in above equations are as:

$$\int_{t_0}^{t_f} \delta V dt = \int_{t_0}^{t_f} \{\delta q\}^T [k_{uu}] \{q\} dt \quad (4.25)$$

$$\int_{t_0}^{t_f} \delta T dt = - \int_{t_0}^{t_f} \{\delta q\}^T [m_{uu}] \{\ddot{q}\} dt \quad (4.26)$$

$$\int_{t_0}^{t_f} \delta W^s dt = \int_{t_0}^{t_f} \{\delta q\}^T \{F_s\} dt \quad (4.27)$$

On putting these values from (4.25), (4.26) and (4.27) in Hamilton equation (4.24) we get

$$\int_{t_0}^{t_f} \left(\{\delta q\}^T \left(-[m_{uu}] \{\ddot{q}\} - [k_{uu}] \{q\} \right) \right) dt = 0 \quad (4.28)$$

On comparing both side coefficient of $\{\delta q\}^T$

$$[m] \{\ddot{q}\} + [k] \{q\} = \{F_s\} \quad (4.29)$$

In global form,

$$[M] \{\ddot{q}\} + [K] \{q\} = \{F\} \quad (4.30)$$

Where

$$[M] = \sum_e [m_e]$$

$$[K] = \sum_e [k_e]$$

$$[F] = \sum_e [F_{se}]$$

For static analysis,

$$[K] \{q\} = \{F\} \quad (4.31)$$

For free vibration analysis, $\{F\}$ is taken zero and hence the equation of motion becomes.

$$[M] \{\ddot{q}\} + [K] \{q\} = \{0\} \quad (4.32)$$

4.5 Patch effect

The above equations can be used for both the isotropic plates and the composite plates. The actuator properties i.e. its voltage characteristics is not considered in the above derivations. The following equations are derived considering the effect of the piezoelectric actuators and sensors.

Assumptions:

1. The piezoelectric actuators/sensors are mounted perfectly over the plate.
2. The voltage applied to the actuator is approximately converted into the force.

Rewriting the displacement components of a composite plate (1) based on the assumptions of the first order deformation theory for small strains.

$$\begin{aligned}
 u(x, y, z, t) &= u_o(x, y, t) + z\theta_x(x, y, t) \\
 v(x, y, z, t) &= v_o(x, y, t) + z\theta_y(x, y, t) \\
 w(x, y, z, t) &= w_o(x, y, t)
 \end{aligned} \tag{4.33}$$

Now the strain vector at any point (x, y, z) with respect to the structural coordinate system can be expressed in a reduced form as

$$\{\varepsilon\} = [T][Z]\{\varepsilon^-\} \tag{4.34}$$

Where

$$[T] = \begin{bmatrix} m^2 & n^2 & 0 & 0 & mn \\ n^2 & m^2 & 0 & 0 & -mn \\ 0 & 0 & m & -n & 0 \\ 0 & 0 & n & m & 0 \\ -2mn & 2mn & 0 & 0 & m^2 - n^2 \end{bmatrix} \tag{4.35}$$

$$[Z] = \begin{bmatrix} 1 & 0 & 0 & 0 & 0 & z & 0 & 0 \\ 0 & 1 & 0 & 0 & 0 & 0 & z & 0 \\ 0 & 0 & 1 & 0 & 0 & 0 & 0 & 0 \\ 0 & 0 & 0 & 1 & 0 & 0 & 0 & 0 \\ 0 & 0 & 0 & 0 & 1 & 0 & 0 & z \end{bmatrix} \tag{4.36}$$

$m = \cos \theta$, $n = \sin \theta$ and θ is the skew angle.

$$\{\varepsilon\} = [\varepsilon_x \varepsilon_y \gamma_{yz} \gamma_{zx} \gamma_{xy}]^T \quad (4.37)$$

$$\left\{ \begin{array}{l} \left(\frac{\partial u_0}{\partial x} \right) \\ \left(\frac{\partial v_0}{\partial y} \right) \\ \left(\frac{\partial w_0}{\partial y} \right) + \theta_y \\ \left(\frac{\partial w_0}{\partial x} \right) + \theta_x \\ \left(\frac{\partial u_0}{\partial y} \right) + \left(\frac{\partial v_0}{\partial x} \right) \\ \theta_{x,x} \\ \theta_{y,y} \\ \theta_{x,y} + \theta_{y,x} \end{array} \right\} = \quad (4.38)$$

Finite Element Model:

An eight noded isoparametric element is adopted and the spatial coordinates in terms of the shape functions are given by

$$x = \sum_{i=1}^8 N_i x_i, \quad y = \sum_{i=1}^8 N_i y_i \quad (4.39)$$

Where N_i are the shape functions

The displacement vector $\{u\}$ at any point $(x, y, 0)$ on the mid plane is defined in terms of the nodal variables and the shape function $[N_d]$ as

$$\{u\} = [N_d] \{u_i\} \quad (4.40)$$

$$[N_d] = [[N_1 I] [N_2 I] \dots [N_8 I]] \quad (4.41)$$

I - a 5x5 Identity matrix

Using the equations (4.34), (4.38) and (4.40) we can write a reduced form of strain vector

$$\{\varepsilon\} = [T][Z][B_d]\{u\} \quad (4.42)$$

$$\text{Where } [B_d] = [[B_1 \ I] [B_2 \ I] \dots [B_8 \ I]] \quad (4.43)$$

and

$$[B_i] = \begin{bmatrix} \frac{\partial N_i}{\partial x} & 0 & 0 & 0 & 0 \\ 0 & \frac{\partial N_i}{\partial y} & 0 & 0 & 0 \\ 0 & 0 & \frac{\partial N_i}{\partial y} & 0 & N_i \\ 0 & 0 & \frac{\partial N_i}{\partial x} & N_i & 0 \\ \frac{\partial N_i}{\partial y} & \frac{\partial N_i}{\partial x} & 0 & 0 & 0 \\ 0 & 0 & 0 & \frac{\partial N_i}{\partial x} & 0 \\ 0 & 0 & 0 & 0 & \frac{\partial N_i}{\partial y} \\ 0 & 0 & 0 & \frac{\partial N_i}{\partial y} & \frac{\partial N_i}{\partial x} \end{bmatrix} \quad (4.44)$$

Energy equations

Internal Work:

Internal work done by the material layer is given by

$$W_{int} = \int_v \{\varepsilon\}^T \{\sigma\} dv \quad (4.45)$$

But the stress is given by

$$\{\sigma\} = [Q]\{\varepsilon\} \quad (4.46)$$

$$\text{Where } [Q] = \begin{bmatrix} \frac{E_1}{1-\nu_{12}\nu_{21}} & \frac{\nu_{12}E_1}{1-\nu_{12}\nu_{21}} & 0 & 0 & 0 \\ \frac{\nu_{12}E_1}{1-\nu_{12}\nu_{21}} & \frac{E_2}{1-\nu_{12}\nu_{21}} & 0 & 0 & 0 \\ 0 & 0 & G_{12} & 0 & 0 \\ 0 & 0 & 0 & G_{23} & 0 \\ 0 & 0 & 0 & 0 & G_{13} \end{bmatrix}$$

From equations (4.45) and (4.46)

$$W_{\text{int}} = \int_v \{\varepsilon\}^T [Q] \{\varepsilon\} dv \quad (4.47)$$

By equation (4.42) and (4.47)

$$W_{\text{int}} = \{u\}^T \int_v [B_d]^T [Z]^T [T]^T [Q] [T] [Z] [B_d] dv \{u\} \quad (4.48)$$

If we say

$$[k_b] = \int_v [B_d]^T [Z]^T [T]^T [Q] [T] [Z] [B_d] dv \quad (4.49)$$

Then, equation (4.48) becomes

$$W_{\text{int}} = \{u\}^T [k_b] \{u\} \quad (4.50)$$

Now considering the stress in the actuator layer,

Internal work done inside the actuator layer can be given as

$$W_{\text{int}}^A = \int_v \{\varepsilon^A\}^T \{\sigma^A\} dv \quad (4.51)$$

But stress in the actuator layer

$$\{\sigma^A\} = [Q^A] \{\varepsilon^A\} - [e] \{E\} \quad (4.52)$$

From equation (4.51) and (4.52) we can write

$$W_{\text{int}}^A = \int_v (\{\varepsilon^A\}^T [Q^A] \{\varepsilon^A\} - \{\varepsilon^A\}^T [e] \{E\}) dv \quad (4.53)$$

By equation (4.36) and (4.42)

$$W_{\text{int}}^A = \{u\}^T \int_v [B_d^A]^T [Z^A]^T [T^A]^T [Q^A] [T^A] [Z^A] [B_d^A] dv \{u\} - \{u\}^T \int_v [B_d^A]^T [Z^A]^T [T^A]^T [e] \{E\} dv \quad (4.54)$$

As the electricity is applied in the thickness direction only

$$\{E\} = \begin{Bmatrix} 0 \\ 0 \\ \frac{\phi_a}{t_a} \end{Bmatrix}$$

$$\text{If } \{E\} = \frac{\phi_a}{t_a} \text{ Then } [e] = \{e_3\}$$

From this and from equation (4.54),

$$W_{\text{int}}^A = \{u\}^T \int_v [B_d^A]^T [Z^A]^T [T^A]^T [Q^A] [T^A] [Z^A] [B_d^A] dv \{u\} - \{u\}^T \int_v [B_d^A]^T [Z^A]^T [T^A]^T [e_3] dA \phi_A \quad (4.55)$$

Say

$$\{k_p\} = \int_v [B_d^A]^T [Z^A]^T [T^A]^T [Q^A] [T^A] [Z^A] [B_d^A] dv \{u\} \text{ and} \quad (4.56)$$

$$\{k_{da}\} = \int_v [B_d^A]^T [Z^A]^T [T^A]^T dA \quad (4.57)$$

Then from equations (4.44), (4.45) and (4.46)

$$W_{\text{int}} = \{u\}^T [k_p] \{u\} - \{u\}^T [k_{da}] \phi_A \quad (4.58)$$

Electric displacement vector is given by the direct piezoelectric effect

$$\{D\} = [e]\{\varepsilon\} + [\kappa]\{E\} \quad (4.59)$$

In the absence of electric field

$$\{D\} = [e]\{\varepsilon\} \quad (4.60)$$

As here strained sensor is only placed in Z direction. Therefore in this case only D_z component of D will be on the sensor surface.

$$\{D_z\} = [e_3]^T \{\varepsilon\} \quad (4.61)$$

From equations (4.42) and (4.61)

$$\{D_z\} = [e_3]^T [T] [Z^S] [B_d^S] \{u\} \quad (4.62)$$

From the Gauss's law, the charge output q_{ij} of the i th electroplated sensor can be given by

$$q^i = \sum_j q_j^i \quad (4.63)$$

Where

$$q_j^i = \int D_z dA \quad (4.64)$$

From equations (4.62) and (4.64)

$$q_j^i(t) = \int \{e_3\}^T [T] [Z^S] [B_d^S] \{u\} dA \quad (4.65)$$

Say $\{k_{ds}\}^T = \int \{e_3\}^T [T] [Z^S] [B] dA$ (4.66)

By equation (4.65) and (4.66)

$$q_j^i(t) = \{k_{ds}\}^T \{u\} \quad (4.67)$$

Current is the rate of change of charge i.e.

$$i = \frac{d}{dt} q_j'(t) \quad (4.68)$$

From equations (4.67) and (4.68)

$$i = \{k_{ds}\}^T \{\dot{u}\} \quad (4.69)$$

Sensor voltage

$$i = g^c \{k_{ds}\}^T \{u\} \quad (4.70)$$

Where g^c is the current gain of the charge amplifier

This sensor voltage is given to the actuator after desired amplification, therefore actuator voltage

$$\phi_A = g \phi_S \quad (4.71)$$

Where g is the constant gain to couple the input actuator voltage and out put sensor,

From equations (4.70) and (4.71)

$$\phi_A = gg^c \{k_{ds}\}^T \{u\} \quad (4.72)$$

By equations (4.58) and (4.72)

$$W_{int} = \{u\}^T [k_p] \{u\} - \{u\}^T [k_{da}] gg^c \{k_{ds}\}^T \quad (4.73)$$

External work done

$$w_{ext} = \int_A \{d\}^T \{f^d\} dA + \sum_i \{d\}^T \{f_i\} - \int_v \{d\}^T \rho \{d\} dv - \int_v \{d\}^T \rho_p \{d\} dv \quad (4.74)$$

$$\text{Where } \{d\} = [ZZ][N][u] \quad (4.75)$$

From equations (4.74) and (4.75)

$$w_{ext} = \{u\}^T \int_A [N]^T \{ZZ\}^T \{f^d\} dA + \{u\}^T [N]^T [ZZ]^T \sum_i \{f_i\} - \{u\}^T \int_v ([N]^T [ZZ]^T \rho [N] + [N]^T [ZZ^A]^T [N]) dv \{u\} \quad (4.76)$$

Now if

$$[m_b] = \int_v [N]^T [ZZ]^T \rho_b [ZZ][N] dv \quad (4.77)$$

$$[m_p] = \int_v [N]^T [ZZ^A]^T \rho_b [ZZ^A][N] dv$$

Where $[ZZ] = \begin{bmatrix} 1 & 0 & 0 & z & 0 \\ 0 & 1 & 0 & 0 & z \\ 0 & 0 & 1 & 0 & 0 \\ 0 & 0 & 0 & 1 & 0 \\ 0 & 0 & 0 & 0 & 1 \end{bmatrix}$

From equations (4.76) and (4.77)

$$w_{ext} = \{u\}^T \int_A [N]^T [ZZ]^T \{f_d\} dA + \{u\}^T [N]^T [ZZ]^T \sum f_i - \{u\}^T [m_b] \{\ddot{u}\} - \{u\}^T [m_p] \quad (4.78)$$

By the principle of virtual work

$$W_{int} = W_{ext} \quad (4.79)$$

This means, from equations (4.50), (4.54), (4.78) and (4.79)

$$[m_b] \{\ddot{u}\} + [m_p] \{\ddot{u}\} + \{k_{da}\} g^c g \{k_{ds}\}^T \{\dot{u}\} + [k_b] \{u\} + [k_p] \{u\} = \int_A [N]^T [ZZ]^T \{f_d\} dA + [N]^T [ZZ]^T \sum \{f_i\} \quad (4.80)$$

In global form,

$$[M_b] \{\ddot{X}\} + [M_p] \{\ddot{X}\} + ([K_{da}] [G_a] [K_{ds}]) \{\dot{X}\} + [K_b] \{X\} + [K_p] \{X\} = \{F^d\} + \{F^p\} \quad (4.81)$$

Say

$$[M] = [M_b] + [M_p];$$

$$[K] = [K_b] + [K_p]; \quad (4.82)$$

$$[F] = [F_b] + [F_p];$$

Assuming a proportional or Rayleigh damping,

$$[C] = \alpha [M] + \beta [K] \quad (4.83)$$

α and β are constants.

From equations (4.81), (4.82) and (4.83)

$$[M] \{\ddot{X}\} + ([C] + [K_{da}] [G_a] [K_{ds}]) \{\dot{X}\} + [K] \{X\} = \{F\} \quad (4.84)$$

Where $[\phi]$ is a normalized eigen vector matrix

Now substituting $[X] = [\phi][Y]$, where $[\phi]$ is the modal matrix

and premultiplying both sides of the equation by $[\phi]^T$, we get

$$[\phi]^T [M] [\phi] \{\ddot{Y}\} + [\phi]^T ([C] + [K_{da}] [G_a] [K_{ds}]) [\phi] \{\dot{Y}\} + [K] [\phi] \{Y\} = [\phi]^T \{F\} \quad (4.86)$$

Now say

$$\begin{aligned} [M_n] &= [\phi]^T [M] [\phi] = \text{diag} [1] \\ [C_n] &= [\phi]^T [C] [\phi] = \text{diag} [2\xi_i \omega_i] \\ [K_n] &= [\phi]^T [K] [\phi] = \text{diag} [\omega_i^2] \end{aligned} \quad (4.87)$$

Now from equations (4.86) and (4.87)

$$[M_n] \{\ddot{Y}\} + ([C_n] + [\phi]^T [K_{da}] [G_a] [K_{ds}] [\phi]) \{\dot{Y}\} + [K_n] \{Y\} = [\phi]^T \{F\} \quad (4.88)$$

$$\{U\} = \{\dot{Y}\} \quad (4.89)$$

From equations (4.88) and (4.89)

$$[M_n] \{\dot{U}\} + ([C_n] + [\phi]^T [K_{da}] [G_a] [K_{ds}] [\phi]) \{U\} + [K_n] \{Y\} = [\phi]^T \{F\} \quad (4.90)$$

From equations (4.88) and (4.89)

$$\begin{Bmatrix} \{\dot{Y}\} \\ \{U\} \end{Bmatrix} = \begin{bmatrix} 0 & I \\ -[M_n]^{-1} [K_n] & -[M]^{-1} ([C_n] + [\phi]^T [K_{da}] [G_a] [K_{ds}] [\phi]) \end{bmatrix} \begin{Bmatrix} \{Y\} \\ \{U\} \end{Bmatrix} + \begin{bmatrix} 0 \\ [\phi]^T \end{bmatrix} \{F\} \quad (4.91)$$

$$[A] = \begin{bmatrix} 0 & I \\ -[M_n]^{-1} [K_n] & -[M]^{-1} ([C_n] + [\phi]^T [K_{da}] [G_a] [K_{ds}] [\phi]) \end{bmatrix}$$

$$[B] = \begin{bmatrix} 0 \\ [\phi]^T \end{bmatrix} \{F\} \quad (4.92)$$

$$\{W\} = \begin{Bmatrix} Y \\ U \end{Bmatrix}$$

4.6 Location Optimization of Point Actuators

The state representation of the model can be written as

From equations (4.91) and (4.92)

$$\{\dot{W}\} = [A] \{W\} + [B] \{F\} \quad (4.93)$$

Note the dependence of matrix B on the location of force actuators. If an actuator is located at the nodal point of a mode, this mode becomes uncontrollable through that actuator. Actuator location in the vicinity of the node would require a large effort to control this mode.

Now, we define the problem of minimum control energy requirement to regulate the system from an initial state, x_0 , to a final state, x_{t_f} as (Hac, and Lui, 1993)

$$\text{Minimize } J_c = \int_0^{t_f} u^T(t)u(t) dt$$

Using Pontryagin's minimum principle

$$(J_c)_{\min} = [e^{A t_f} x(0) - x(t_f)]^T W_c(t_f)^{-1} [e^{A t_f} x(0) - x(t_f)]$$

where

$$W_c(t_f) = \int_0^{t_f} e^{A \tau} B B^T e^{A^T \tau} d \tau$$

The matrix $W_c(t_f)$ is called the controllability grammian matrix and it depends upon the input matrix B . Maximizing a norm of the controllability grammian matrix would lead to the minimum control energy requirement. In addition, a small eigenvalues of the controllability grammian matrix would lead to at least one mode requiring very high control effort. This implies that all the eigenvalues of the controllability grammian matrix should be as high as possible. It is also more desirable to have the condition of minimum energy requirement be independent of the final time, t_f . A grammian matrix independent of t_f is obtained using the following relation: [Jha A.K.,2002]

$$W_c(t_f) = W_c(\infty) - e^{A t_f} W_c(\infty) e^{A^T t_f}$$

For a stable system, as t_f increases, the effect of the second term in the above equation decreases and hence it is appropriate to impose the minimization problem based upon $W_c(\infty)$, which is independent of the final time. The matrix $W_c(\infty)$ can be calculated by solving the Lyapunov equation

$$A W_c(\infty) + W_c(\infty) A^T = -[Q] \tag{4.94}$$

where

$$[Q] = \begin{bmatrix} K_n & 0 \\ 0 & M_n \end{bmatrix}$$

The eigenvalues of the matrix $W_c(\infty)$ play a crucial role in determining the performance of the actuator. Based upon the observations about the eigenvalues, we define the following performance index (PI_c)

$$PI_c = \frac{1}{\sigma(\lambda_i)} \left(\sum_{i=1}^{2N} \lambda_i \right) \sqrt[2N]{\prod_{i=1}^{2N} (\lambda_i)} \quad (4.95)$$

where λ_i are the eigenvalues of $W_c(\infty)$, and $\sigma(\lambda_i)$ is the standard deviation of λ_i . A high value of the standard deviation implies that the eigenvalues are widely separated and hence some of them are less controllable and some of them are more controllable. A case where all the modes are almost equally controllable is preferable. This leads to a very low standard deviation and hence a high performance measure. The summation term in PI_c represents the size of the grammian and should be large for good performance. To ensure that all the eigenvalues of the grammian are high (for good controllability of each mode), the performance index includes the product of all the eigenvalues.

Chapter 5. GENETIC ALGORITHMS

Once the governing equations are derived, the genetic algorithms are used to optimize the location of actuators. The genetic algorithms require an objective function for optimization. The minimizing of dissipation of energy explained in the previous chapter is taken as the objective function for this optimizing technique. This chapter explains the development of genetic algorithms and the various variables used in the algorithm. The steps of genetic algorithms are discussed separately in detail in this chapter.

5.1 Description

Genetic Algorithms were developed by Holland in 1975. Although these algorithms emerged simultaneously with two other streams known as Evolution Strategies (ES) and Evolutionary Programming (EP), GAs are today the most widely known type of evolutionary algorithms. Differing from conventional search techniques, the common feature of these algorithms is to simulate the search process of natural evolution and take advantage of the Darwinian survival-of-the fittest principle. In short, Evolutionary algorithms start with an arbitrarily initialized population of coded individuals, each of which represents a search point in the space of potential solution. The goodness of each individual is evaluated by a fitness function which is defined from the objective function of the optimization problem. [Garcia, 1999]

Then, the population evolves toward increasingly better regions of the search space by means of both random and probabilistic (or deterministic in some algorithms) biological operations.

The basic operators used in GAs consist of selection (the selection of parents for breeding), crossover (the exchange of parental information to create children) and mutation (the changing of an individual). In addition, following the Darwinian Theory, an elitism operator (the protection of best individuals) is found in more elaborated GAs.

Note however here that the ergodicity of the biological operators used in GAs makes them potentially effective at performing global search (in probability). Also, GAs

have the attribute of a probabilistic evolutionary search (although it is most commonly referred to as a randomized search), and are neither bound to assumptions regarding continuity nor limited by required prerequisites.

The GA technique has been theoretically and empirically proven to provide robust searches in complex spaces. Much of the early work of GAs used a universal internal representation involving fixed-length binary chromosomes with binary genetic operators.

Consequently, most of the theory developed (which could fill several volumes!) is based on binary coding. In developing the Fundamental Theorem of GAs, Holland (1975) focused on modeling ideal Simple GAs (SGAs) to better understand and predict GA behavior with above-average fitness receive exponentially increasing trials in subsequent generations. Many properties in terms of the binary genetic operator's effectiveness were concluded from this theorem. However, it is pointed out that these properties give some limited insight into the GA behavior. Mitchell believes that a more useful approach to understanding and predicting GA behavior would be analogous to that of statistical mechanics in physics whose traditional goal is to describe the laws of physical systems in terms of macroscopic quantities, such as pressure and temperature, rather than in terms of the microscopic particles (molecules) making up the system. Such an approach will aim at laws of GA behavior described by more macroscopic statistics such as "mean fitness in the population" or "mean degree of symmetry in the chromosomes" rather than keeping track of the huge number of individual components in the system (e.g., the exact genetic composition of each population). Regarding theoretical guidelines about which GA to apply, the real problems encountered by GAs usually compel tailoring the GA at hand as the use of different encoding and operator variants could provide different solutions.

One realizes that there are therefore no rigorous guidelines for predicting which variants and more particularly, which encoding, works the best. By addressing the binary/floating point debate, the work it is confirmed that there is no best approach and that the best representation depends on the problem at hand.

As one can understand, there are many controversies in the GA community over the approaches used, revealing that GA theory is by no means a closed book (indeed, there are more open questions than solved ones). One final point worth mentioning about the GA theory is that many of today's algorithms show enormous differences to the original SGA. [Garcia, 1999]

5.2 Fundamentals

The purpose here is not to give a thorough theoretical analysis of the GAs mechanism, as there are excellent introductory tutorials in the literature. Instead, the objective of this section is to provide some answers to explicit questions one may have about GAs. In the following, the structure of a simple GA will be presented along with a general overview of the main techniques/variants that are employed in the GA process. Then, the most important features which differentiate GAs from conventional optimization techniques are described. Eventually, the strengths and weaknesses of GAs are outlined and the type of problems for which the use of these algorithms is pertinent is indicated.

5.3 What are GAs?

Like all evolutionary algorithms, a GA is a search procedure modeled on the mechanics of natural selection rather than a simulated reasoning process. These algorithms were originally used for the study of artificial systems. Since their inception GAs have been subject to a growing interest as an optimization technique in nearly all kinds of engineering applications. Today, there are so many different GAs that it turns out, there is no rigorous definition of GAs accepted by all in the evolutionary computation community that differentiates GAs from other evolutionary computation methods. Indeed, some currently used GAs can be very far from Holland's original conception. However, it can be said that most methods called "GAs" have at least the following elements in common: populations of individuals, selection according to the individuals' fitness, crossover to produce new individuals, random mutation of new individuals, and replacement of the populations. These elements are illustrated next, in the description of how a simple GA works. A typical GA flowchart appears in Fig. 5.1.

How do GAs work?

GAs are based on the collective learning process within a population of individuals (trial solutions called chromosomes), each of which represents a search point in the space of potential solutions to a given problem. The chromosomes code a set of parameters (called genes). The population (of size n_s) is generally randomly initialized (at the generation $n_g=0$) in the parametric search space (see POP0 in Fig.5.1). The individuals are evaluated and ranked in terms of a fitness function. Then, the population evolves towards fitter regions of the search space by means of the sequential application of genetic operators.

The basic operators of a simple GA consist of selection (selection of parents for breeding), crossover (mating of parents to create children) and mutation (random changing of a gene). Following the Darwinian theory of survival of the fittest, an elitism operator is usually found in the generational replacement. A generation is accomplished when the sequence defined by the application of all operators to the individual parents is performed, as illustrated in Fig. 5.1. The GA produces as many generations as necessary until the convergence criterion is reached. The goal, throughout this process of simulated evolution, is to obtain the best chromosome in the final population to be a highly evolved solution to the problem.

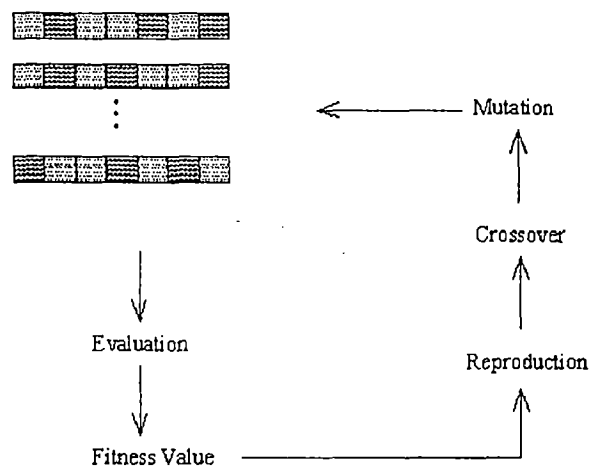


Figure-5.1: Typical Genetic algorithm

5.4 Basic steps in a Genetic Algorithm

5.4.1 Encoding scheme

To enhance the performance of a GA, a chromosome representation that stores problem specific information is desired. Although GAs were developed to work on chromosomes encoded as binary strings, it is today common knowledge that for numerical optimization problems, one should use a GA with floating point representation. One important point that may, however, not be obvious when one starts to use GAs (which was my case) is that the crossover variants used should be appropriate to the encoding used. There indeed exist both conventional (binary) and arithmetical crossover techniques to fit the two different representations. Note that when using the real representation, a chromosome is a vector of np genes for the np parameters. It should be emphasized here that because much of the early work of GAs used a universal coding involving abstract binary chromosomes (that needed to be decoded), research on GAs has been slow to spread from computer science to engineering, and very little theory exist in the literature on real-valued encoding. [Garcia, 1999]

5.4.2 Fitness function

The fitness plays the role of the environment in which the chromosomes are to be evaluated. This is thus a crucial link between the GA and the system. This function can be simply taken as the objective function to optimize or as a transformation (scaling) of it. It is assumed that the fitness function to be optimized is positive. In cases where the objective function happens to be negative, the fitness function will be a transformation of the objective function.

5.4.3 Parent selection

Basically, the selection operator determines which of the individuals in the current population (of size ns) will be allowed to pass their genetic material to the next generation. Using the GA language, one says that it builds up the mating pool by

selecting n_s individuals from the current population. There are many ways to achieve effective selection, including proportionate, ranking and tournament schemes. The key assumption is to give preference to fitter individuals. Using fitness proportionate selection, the number of times an individual is expected to reproduce is equal to its fitness divided by the average of fitnesses in the population. The most popular and easiest mechanism is the Roulette wheel selection where each chromosome in the current population has a Roulette wheel slot sized in proportion to its fitness. However, depending on the environment (fitness), proportionate and ranking selection schemes may lead to premature convergence or on the contrary, to a slow finishing. Those are well-known severe technical problems of GAs. However, both problems can be avoided if scaled fitness values are used instead of the original values. Another way to circumvent these problems is to use a more adequate selection operator. In many applications, tournament selection has proved to yield superior results to fitness rank selection. In the simplest form, the so-called binary selection, two chromosomes are selected randomly from the current population but only the one with the higher fitness value is inserted into the mating pool with a probability p_t . One interesting feature about this selection scheme is that one can adjust the selection pressure directly from the tournament probability p_t (typically larger than 0.5). Regardless of which selection technique is used, the selection operator produces an intermediate population, the mating pool, which consists only of individuals that are members of the current population. The following two operators, crossover and mutation, are then applied to this mating pool in order to generate children.

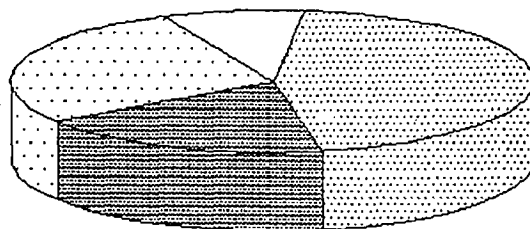


Figure 5.2: Roulette wheel

5.4.4 Crossover

The crossover operator is the key operator to generate new individuals in the population. In addition, it has been shown in the literature that so-called “deceptive” problems can be made “easy” by the use of an appropriate definition of the crossover function. This operator is applied to each pair of the mating pool with a crossover probability p_c , usually taken from $[0.6,1]$, to produce one or two children. With probability $1-p_c$, no changes are made to the parents (they are simply cloned), but with probability p_c , genetic material is exchanged between the two parents. In the simplest crossover, the single point crossover, a crossover point is randomly selected and the portions of the two chromosomes beyond this point are exchanged. Multipoint crossover is similar except that multiple cross points are chosen at random with no duplication. Uniform crossover generalizes the scheme by making every gene a potential crossover point. Single, multipoint and uniform crossovers are generally considered conventional binary techniques, and when real encoding is used, arithmetic crossovers are the most suited.

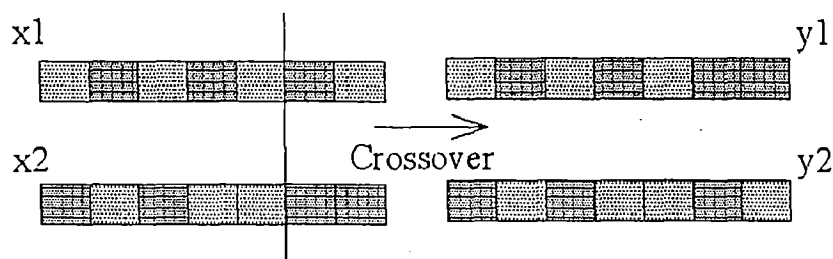


Figure 5.3: Crossover

5.4.5 Mutation

This operator should allow a GA the finding of solutions which contain genes that are nonexistent in the initial population. It can also prevent the GA from losing some genetic material without any chance of adopting it again. Often viewed as a background operator, mutation modifies gene values according to a mutation probability. Using binary encoding, this simply means changing a 1 to a 0 and vice versa with a small probability. Using real encoding, when a global modification called jump mutation is applied, each gene in any chromosome is replaced with a random value (from the entire

parametric search space) with probability pmj . A “mutation-based” operator can also be applied locally with the creep variant (not a pure mutation operator in the sense of GAs) which consists in the addition or subtraction with probability pmc of a small value to the gene (1% of the actual gene value).

Whereas the crossover operator reduces the diversity in the population, the mutation operator increases it again. The higher the mutation probability, the smaller is the danger of premature convergence. A high mutation probability will however transform a GA into some kind of random search algorithm, which is of course not the intention of the algorithm! Mutation probabilities are usually small (so as not to interfere with the combination of the best features of parents made by the crossover operation), and range from 0.001 to 0.10, the higher values being typically applied with real encoding.

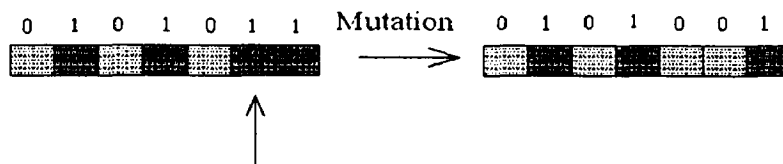
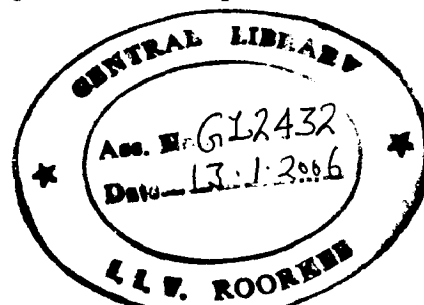


Figure 5.4: Mutation

5.4.6 Replacement strategies

In the simplest form of GAs, when the operation of selection, crossover and mutation are completed on the ns individuals of the current population, this entire population is replaced with the children created. This is the traditional generational replacement. Variations where not all individuals are replaced in each generation exist. The simplest case of such a strategy is the elitist strategy where the individual with the highest fitness (according to the Darwinian theory of survival of the fittest) is directly transferred from the old to the new generation and only the other $ns-1$ children are generated by the application of genetic operators.

Generational replacement with probability pr is often used in which $ns \times pr$ parents are replaced with children while the $ns \times (1-pr)$ best parents are kept. An alternative to



replacing an entire population at once is to replace one organism in the population whenever a new organism is created. This variant is known as a steady-state GA.

5.4.7 Convergence criterion

The most widely used stopping conditions are either that a given number of generations have been done already, or that the population has become uniform. When the condition is chosen, GAs are typically iterated for anywhere from 10 to 500 or more iterations. User defined convergence criterion that are better suited to the problem to be solved should be preferred (although most of the studies do not address this problem) but it is however not easy to define such a criterion, as it will be shown in this work.

5.4.8 Performance criterion

What does it mean for a GA to perform well or poorly? Some performance criteria can provide answers to this question. The best fitness reached (best-so-far) is a typical one. One criterion for computational cost is the number of function evaluations. Indeed, in almost all GA applications, the time to perform a function evaluation usually exceeds the time required to execute other parts of the algorithm (which are considered to take negligible time). Note that because randomness plays a large role in each run (two runs with different random number seeds will generally produce different outputs), often GA researchers report statistics (about the best fitness for instance) averaged over many different runs of the GA on the same problem.

Besides the genetic operators presented here, there exist a number of different operators (inversion, reordering), in addition to advanced features (diploid, dominant and recessive genes, sharing fitness function) which are used in different applications but are not yet widely used. GAs are still far from maturity.

Chapter 6. RESULTS AND DISCUSSION

A MATLAB code is written and has been used to solution for various static and dynamic problems. The variation of max static deflection with various parameters of the laminate laminated plates has been studied and a free vibration analysis of isotropic and orthotropic is carried out using the code to obtain the natural frequencies and mode shapes.

In actual terms, the plate is a structure which has infinite number of degrees of freedom. So it can have any number of natural frequencies. But we are concerned with the lower frequencies which come in practical limits. Here with the use of finite elements (grid: 2 x 2 in most of the cases, resulting in 3 X 3=9 nodes) we are reducing the degree of freedom of the plate to a total of 45 degrees of freedom which include 5 degrees of freedom($u, v, w, \theta_x, \theta_y$) at each node.

Further when we apply the boundary conditions or supports, depending upon the type of support applied, some more DOF's are constrained resulting in a fewer degrees of freedom left for calculating the natural frequencies and mode shapes.

The following figures show the 2 x 2 FE model for a simply supported, cantilever and clamped plate with constraints at the boundaries.

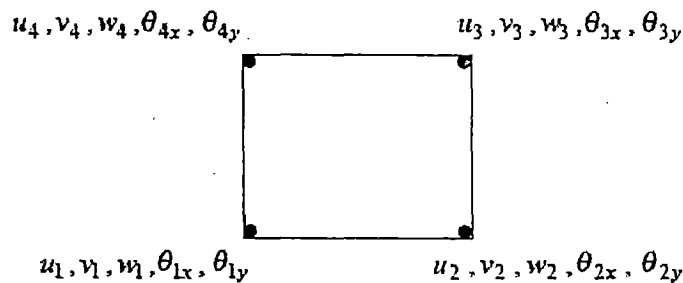


Figure 6.1: DOFs at each node

6.1 Boundary Conditions

6.1.1 Simply supported plate:

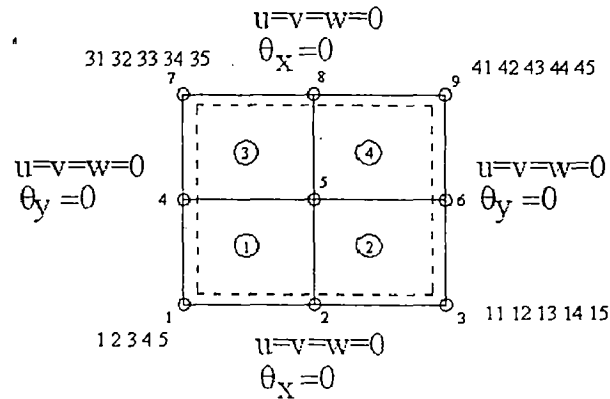


Figure 6.2: Boundary conditions for a simply supported plate.

After applying the boundary conditions [ref 4.2], out of 45 DOFs, we will get 38 DOFs as zeros. i.e. DOFs

1 2 3 4 5 6 7 8 9 11 12 13 14 15 16 17 18 20 21 22 26
27 28 30 31 32 33 34 35 36 37 38 39 41 42 43 44 45

will be zeros, and we will be left with DOFs 10 19 23 24 25 29 40 with some values.

That is we will be left with only 7 DOFs. So in dynamic analysis of a simply supported plate we will get 7 natural frequencies and corresponding mode shapes in the dynamic analysis.

6.1.2 Cantilever plate:

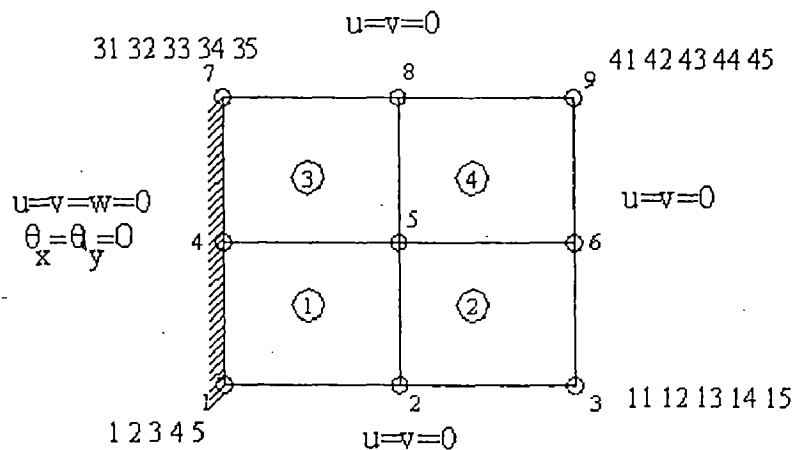


Figure 6.3: Boundary conditions for a cantilever plate

After applying the boundary conditions [ref. 4.2], out of 45 DOFs, we will get 27 DOFs as zeros.

i.e. DOFs

1 2 3 4 5 6 7 11 12 16 17 18 19 20 21 22 26 27 31 32
33 34 35 36 37 41 42

will be zeros,

and we will be left with DOFs 8 9 10 13 14 15 23 24 25 28 29 30 38 39 40 43 44 45 with some values.

That is we will be left with only 18 DOFs. So for a simply supported plate we will get 18 natural frequencies and corresponding mode shapes in the dynamic analysis.

6.1.3 Clamped plate:

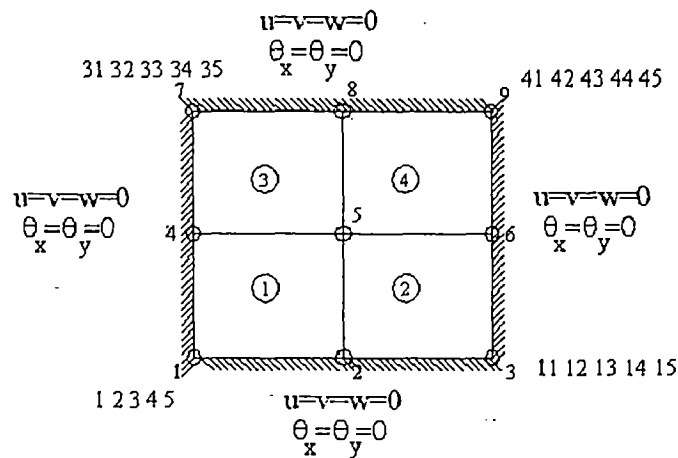


Figure 6.4: Boundary conditions for a clamped plate

After applying the boundary conditions [ref. 4.2], out of 45 DOFs, we will get 42 DOFs as zeros.

i.e. DOFs

1 2 3 4 5 6 7 8 9 10 11 12 13 14 15 16 17 18 19 20 21
22 26 27 28 29 30 31 32 33 34 35 36 37 38 39 40 41 42 43 44
45

will be zeros,

and we will be left with DOFs 23 24 25 with some values.

That is we will be left with only 3 DOFs. So for a clamped plate we will get 3 natural frequencies and corresponding mode shapes in the dynamic analysis.

6.2 Static analysis results

6.2.1 Effect of grid size on max deflection of the plate.

The program was run to obtain the results using different grid sizes (or refinement of mesh) for different boundary conditions.

Material Properties:

$$E_1 = 30 \times 10^6 \text{ N/m}^2$$

$$E_2 = 30 \times 10^6 \text{ N/m}^2 \text{ (isotropic material)}$$

$$\nu = 0.3$$

$$G_{12} = E_1 / (1 + \nu) = G_{13} = G_{23};$$

Geometric Properties:

Plate dimensions: 10m x 10m x .1m

Load = 500 N

Density: 2752.3 Kg/ m³

Sl.No	Grid	Max Deflection Simply Supported plate (m)	Max Deflection Cantilever plate (m)	Max Deflection Clamped Plate (m)
1	2 x 2	0.1662	4.7740	.0037
2	4 x 4	0.1446	4.7066	.0868
3	6 x 6	0.1466	4.6982	.0795
4	8 x 8	0.1472	4.6976	.0823
5	10 x 10	0.1475	4.6978	.0841

Table 6.1: Deflections for different grid sizes for plate with different boundary conditions

The table 6.1 shows the values of the deflection obtained by solving the problem considering the different grid sizes, in other words the number of elements and the figures 6.5, 6.6 and 6.7 show the same graphically for different boundary conditions for the plate.

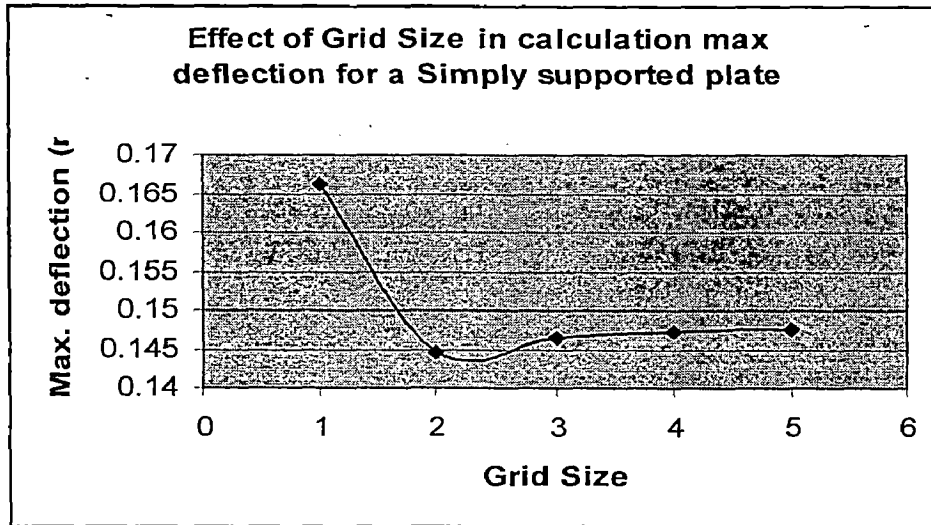


Figure 6.5: Max. deflection obtained considering different grid sizes for a simply supported plate

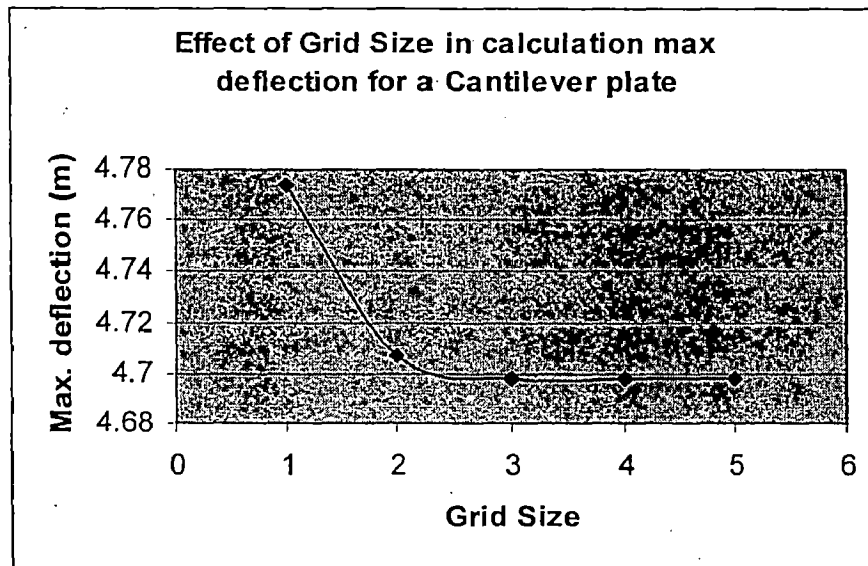


Figure 6.6: Max. deflection obtained for different grid sizes for a cantilevered plate

It was observed that the use of small number of elements resulted in large deviation of the results obtained from the actual results. As we can see from the above results the use of 1x1 has a large deviation and while 2x2 has a small. However as we go on increasing the size of the grid i.e. increase the number of elements, the results converge and are approximately equal to the actual results as we can see from the above results and graphs the use of higher grids 3x3, 4x4, 5x5 have almost equal value for the deflection.

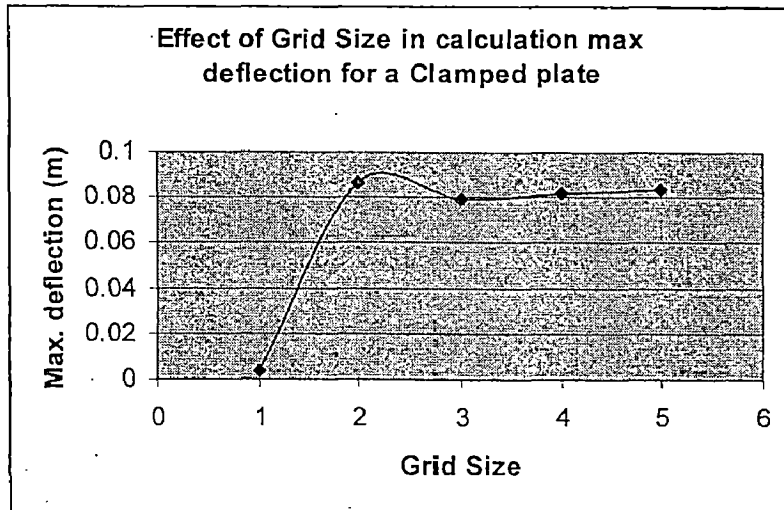


Figure 6.7: Max deflection obtained for different grid sizes for a clamped plate

6.2.2 The effect of fiber orientation in an orthotropic material on maximum static deflection.

The program was executed to obtain the results using different fiber orientation angles for different boundary conditions.

Material Properties:

$$E_1 = 1 \times 10^6 \text{ N/m}^2$$

$$E_2 = 30 \times 10^6 \text{ N/m}^2$$

$$\nu = 0.3$$

$$G_{12} = E_1 / (1 + \nu) = G_{13} = G_{23};$$

$$\text{Density: } 2752.3 \text{ Kg/m}^3$$

Geometric properties:

Plate dimensions: 10m x 10m x .1m

Load = 500 N

Density: 2752.3 Kg/m³

The material properties and geometric properties of the plate are stated above. The table 6.2 gives the deflections for different orientation angles in a composite plate for a simply supported and a cantilevered plate.

Sl. No	Orientation of fiber (degrees)	Max deflection Simply supported plate (m)	Max deflection Cantilever plate (m)
1	0	0.5606	5.5126
2	15	0.5245	5.2145
3	30	0.4646	4.6158
4	45	0.4394	4.5125
5	60	0.4646	4.4849
6	75	0.5606	4.1226
7	90	0.5606	3.5126
8	105	0.5245	4.1312
9	120	0.4646	4.5016
10	150	0.4646	4.7012
11	180	0.5606	5.2541

Table 6.2: Deflections for different orientation angle of the fibers for a simply supported and cantilevered plate

It was observed that for simply supported plate the deflection was found to be maximum for orientation angles 0, 45 and 90 degrees, which means that the plate offers minimum stiffness at these orientation angles. Whereas the deflection is minimum for angle 22.5 and 67.5 degrees. It means the plate offers maximum stiffness when the fibers are oriented at these angles. The following figures 6.8 and 6.9 shows the change in deflection with respect to the change in orientation angle of the fibers graphically for a simply supported plate and a cantilevered plate respectively.

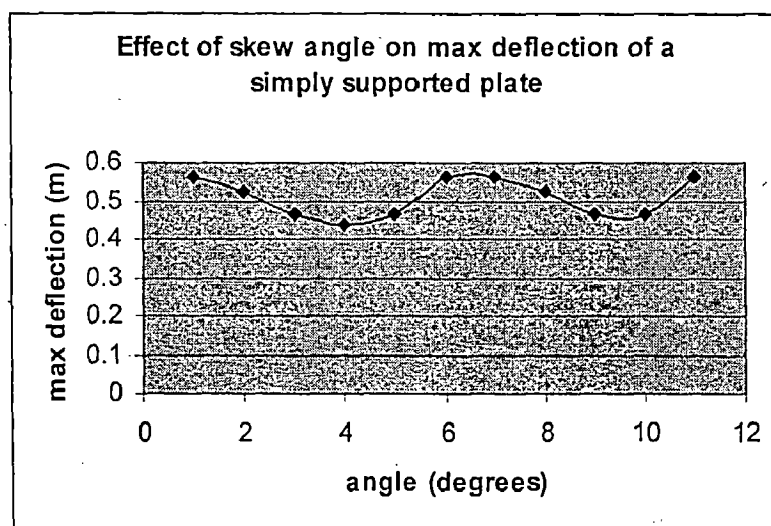


Figure 6.8: Variation of max deflection with the orientation angle: simply supported plate

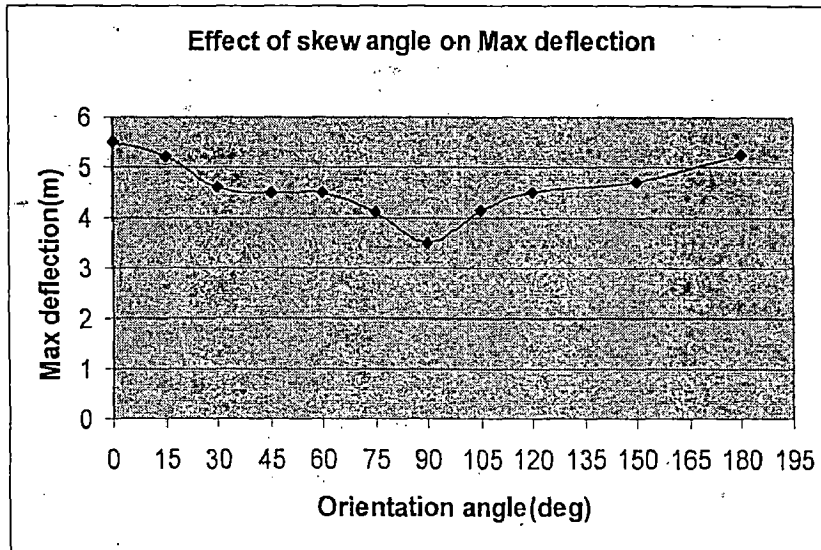


Figure 6.9: Variation of Max deflection with the orientation angle: cantilever plate

6.2.3. Effect of h/L on maximum deflection for a cross ply laminated plate which is simply supported.

The program was executed to obtain the results using different fiber orientation angles for different boundary conditions.

No. of layers= 9

Lamination pattern: 0/90/0/90/0/90/0/90/0

Material Properties:

All layers of same material

$$E_1 = 0.3 \times 6.8948 \times 10^{11} \text{ N/m}^2$$

$$E_2 = 0.75 \times 6.8948 \times 10^9 \text{ N/m}^2$$

$$\nu = 0.3$$

$$G_{12} = 0.45 \times 6.8948 \times 10^9 \text{ N/m}^2 = G_{23}$$

$$G_{13} = 0.375 \times 6.8948 \times 10^9 \text{ N/m}^2$$

Density: 1510 Kg/ m³

Geometric Properties:

Plate dimensions: 10m x 10m x .1m

Load = 500 N

Sl. No	h/ a	2 X 2	4 X 4	6 X 6
1	0.1	0.419	0.4255	0.4265
2	0.05	0.4024	0.4095	0.4055
3	0.01	0.3971	0.4044	.0.4106
4	0.001	0.3969	0.4041	0.4053
5	0.0001	0.3969	0.4041	0.4053
6	0.00001	0.3969	0.4041	0.4053

Table 6.3: Deflections for different thickness to side length ratios for a simply supported plate using different grid sizes.

Table 6.3 gives the values of the deflection for different thickness to side length ratio of a simply supported square plate obtained using various grid sizes. As expected it was observed that the deflections were least when the thickness of the plate is minimum and as we go on increasing the thickness the stiffness of the member increases and the deflection for the applied load decreases. The following figure 6.10 shows this graphically.

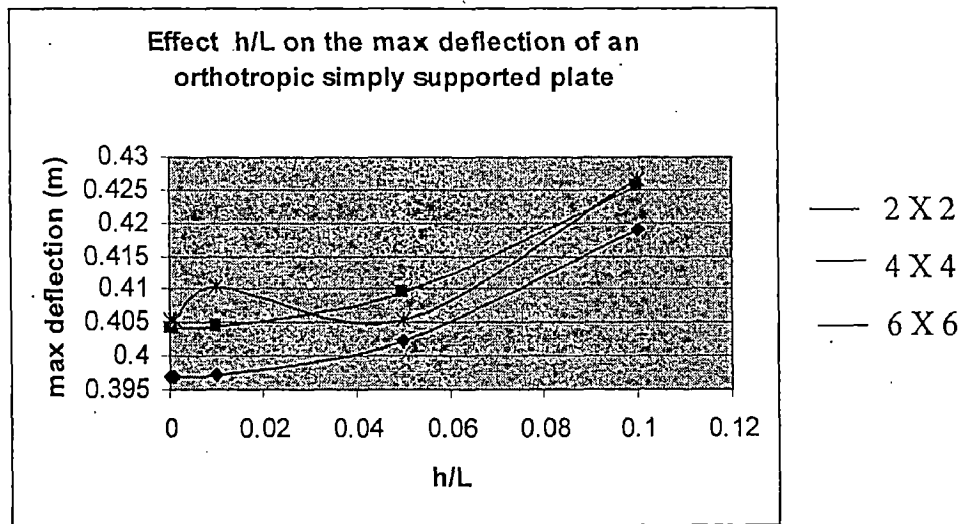


Figure 6.10: Variation of Max deflection with the thickness of plate : simply supported plate

6.3 Dynamic analysis results:

6.3.1. Dynamic analysis of isotropic plate:

After executing the program for dynamic analysis we obtain the natural frequencies of the plate. We have used an element grid size of 4X4.

No. of layers: 1

Material properties of the plate:

$$E_1 = 30 \times 10^6 \text{ N/mm}^2$$

$$E_2 = 30 \times 10^6 \text{ N/mm}^2 \text{ (isotropic material)}$$

$$\nu = 0.3$$

$$G_{12} = E_1 / (1 + \nu) = G_{13} = G_{23}$$

$$\text{Density: } 2752.3 \text{ Kg/m}^3$$

Geometry properties of the plate:

$$W = 10;$$

$$L = W;$$

$$h = L/10$$

Case1. Simply supported plate:

Mode No.	Natural frequency(Hz)
1	1.2405
2	12.4345
3	13.5984
4	25.5588
5	26.4842
6	29.0095
7	29.8524

Table 6.4: Natural frequencies for an isotropic simply supported plate

Case 2: Clamped plate

Mode No.	Natural frequency(Hz)
1	4.0701
2	25.8808
3	25.8808

Table 6.5: Natural frequencies for an isotropic clamped plate

Case 3: Cantilever plate:

Mode No.	Natural Frequency(Hz)
1	0.1741
2	0.4446
3	1.2834
4	1.5693
5	1.7986
6	2.0090
7	7.6769
8	11.9636
9	12.0564
10	13.2627
11	19.1503
12	19.7475
13	20.5032
14	21.9353
15	28.5818
16	29.3585
17	32.5296
18	32.6847

Table 6.6: Natural frequencies for an isotropic cantilever plate

6.3.2. Dynamic analysis of orthotropic plate:

No of layers: 2

Material Properties:

$$E_2(i) = 30 \times 10^6 \text{ N/m}^2$$

$$E_1(i) = 1200 \times 10^6 \text{ N/m}^2$$

$$\nu_{12}(i) = 0.25;$$

$$G_{12} = 18 \times 10^6 \text{ N/m}^2 ;$$

$$G_{13} = 15 \times 10^6 \text{ N/m}^2 ;$$

$$G_{23} = 15 \times 10^6 \text{ N/m}^2 ;$$

$$\text{Density} = 2752.3 \text{ kg/m}^3;$$

$$\text{Petteren}=[0,90] \quad i=1,2;$$

Geometry properties of the plate:

$$W = 1\text{m};$$

$$L = W;$$

$$h = L/10$$

$$\text{Thicknesses of the layers} = [h, h]$$

6.3.2.1 Natural frequencies:

Case1. Simply supported plate:

Mode No.	Natural frequency(Hz)
1	56.4
2	600.4
3	606.4
4	648.2
5	748.7
6	769.6
7	1063.0

Table 6.7: Natural frequencies for an orthotropic simply supported plate

Case 2: Clamped plate

Mode No.	Natural frequency(Hz)
1	84.5961
2	646.8550
3	747.1693

Table 6.8: Natural frequencies for an orthotropic clamped plate

Case 3: Cantilever plate:

Mode No.	Natural Frequency(Hz)
1	14.2926
2	15.8610
3	60.3229
4	72.4961
5	72.9922
6	78.6176
7	291.6285
8	421.8742
9	535.4848
10	642.9015
11	672.8936
12	703.8637
13	723.0361
14	766.3846
15	776.2318
16	875.7813
17	933.7300
18	952.3341

Table 6.9: Natural frequencies for an orthotropic cantilever plate

6.3.2.2 Mode shapes

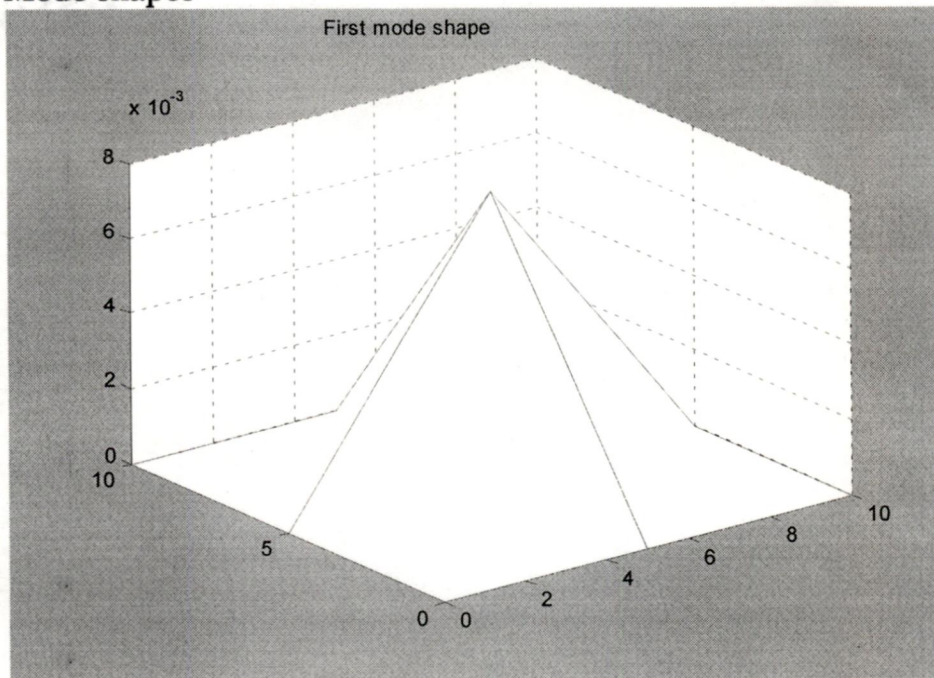


Figure 6.11: 1st Mode shape: Simply supported orthotropic plate

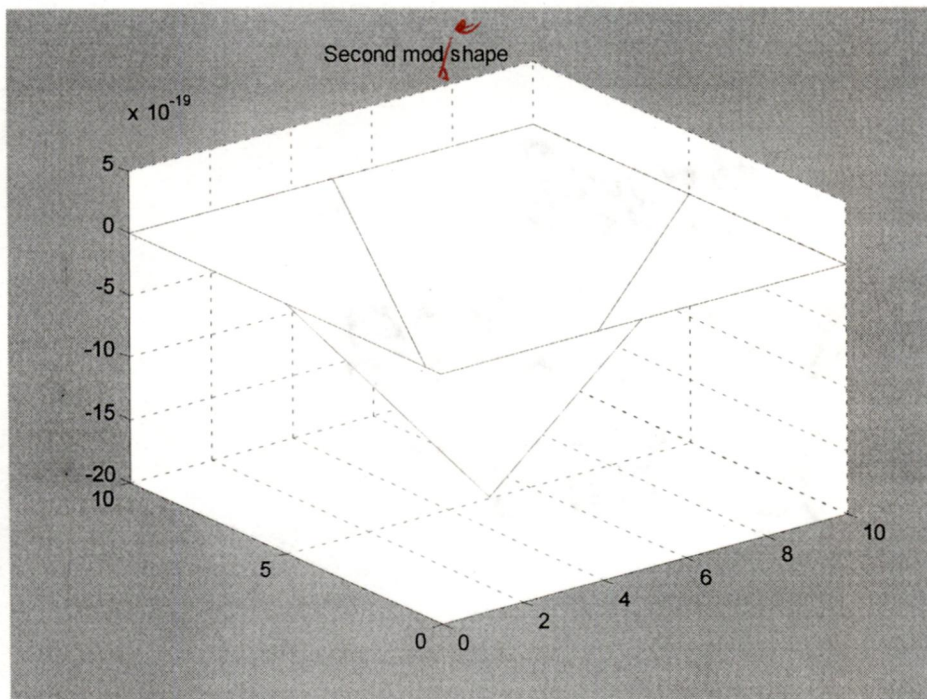


Figure 6.12: 2nd Mode shape: Simply supported orthotropic plate

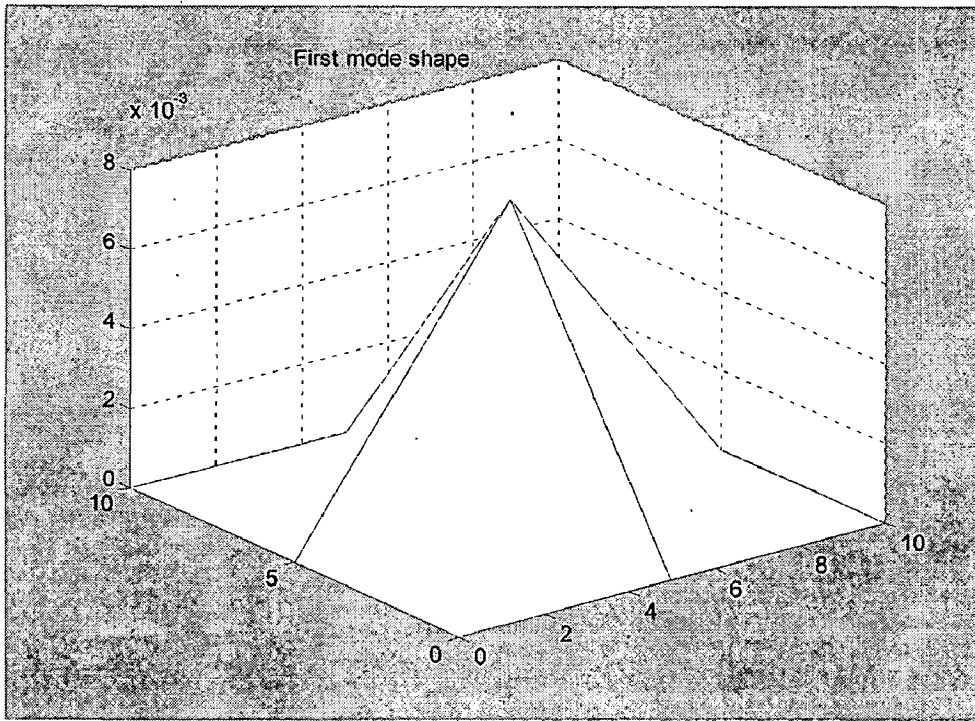


Figure 6.13: 1st Mode shape: Clamped orthotropic plate

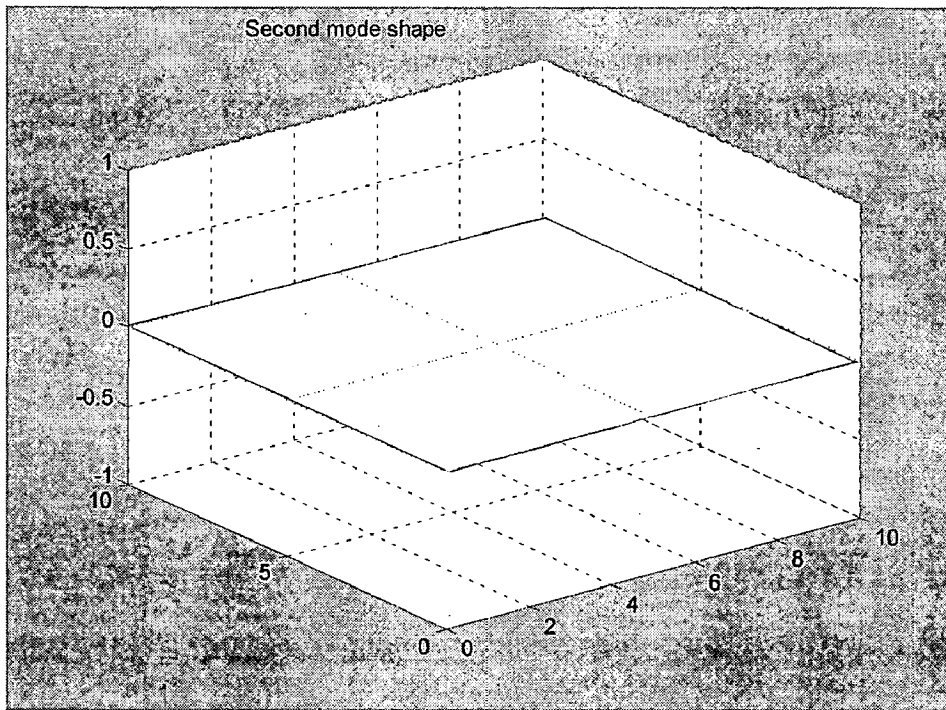


Figure 6.14: 2nd Mode shape: Clamped orthotropic plate

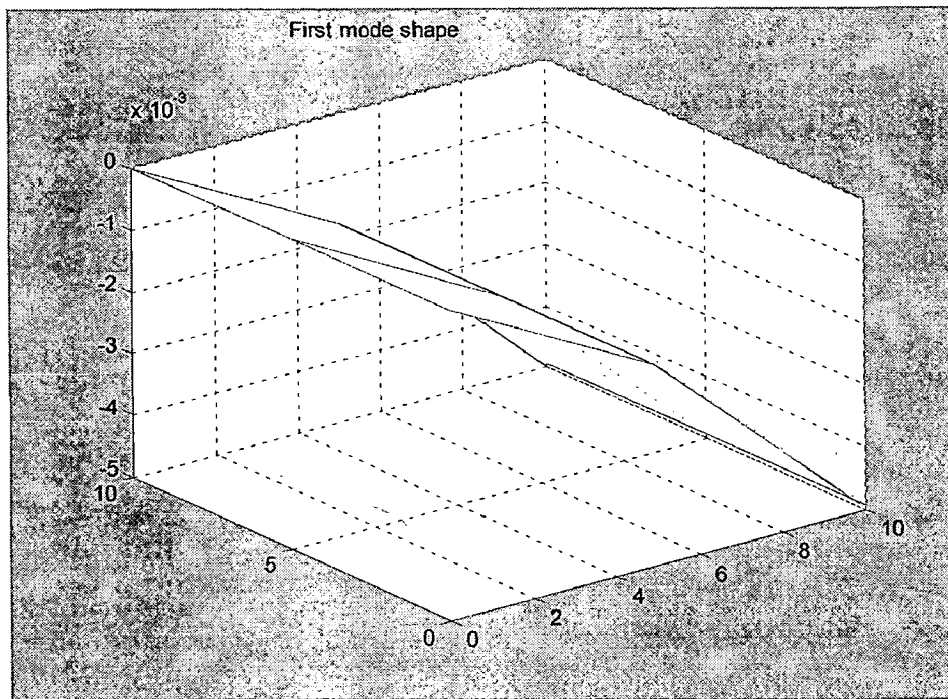


Figure 6.15: 1st Mode shape: Cantilevered orthotropic plate

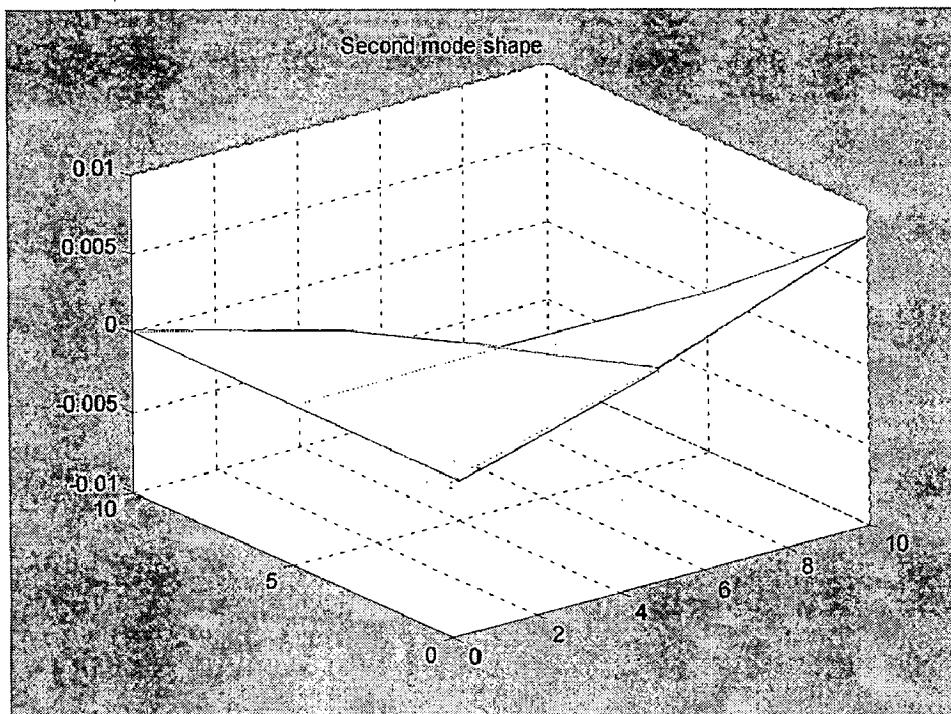


Figure 6.16: 2nd Mode shape: cantilevered orthotropic plate

6.3.3. Variation of natural frequencies with the orientation angle for a cantilevered plate:

The above plate is considered to study the how the natural frequency varies as the orientation angle of the fiber in the composite material changes. The material properties and geometric properties are taken from the previous problem.

Sl No.	Orientation angle (deg)	Natural Frequency (Hz)
1	0	14.2926
2	15	14.6125
3	30	15.2341
4	45	15.6213
5	60	15.2362
6	75	14.6201
7	90	14.3005

Table 6.10: First natural frequencies for a cantilevered plate for different orientation angles

It was observed that for an orthotropic plate, the natural frequency increases with increase in the orientation angle from 0 and then decreases.

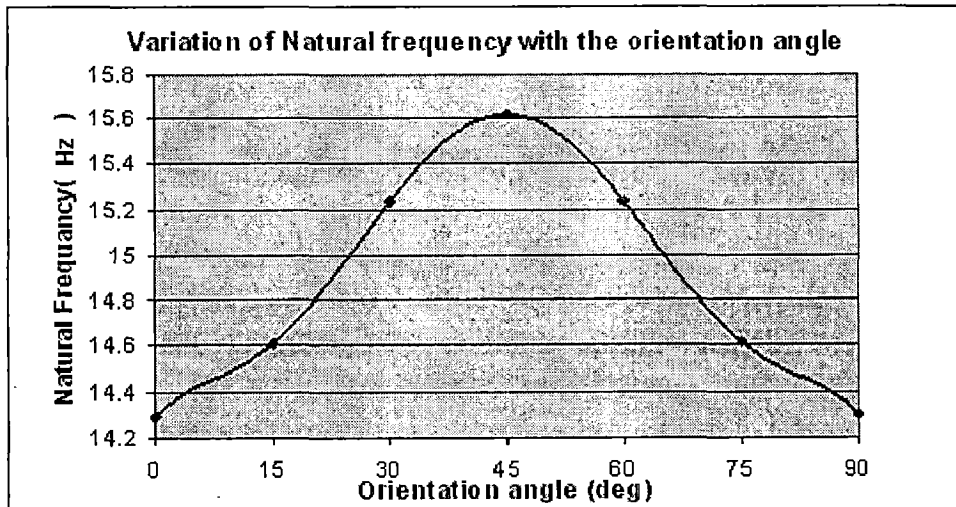


Figure 6.17: The variation of first natural frequency with orientation angle for a cantilevered orthotropic plate

The natural frequency is minimum when the orientation angle is 0 degrees. It increases with the increase in the angle up to 45 degrees, and then decreases in the same manner till 90 degrees. We can conclude from the results that the plate offers minimum stiffness when the orientation angle of the fibers is 0 degrees or 90 degrees that is when they are along the coordinate axes, and maximum stiffness when the fibers are oriented

at an angle 45 degrees. The values of first natural frequencies are tabulated in table 6.10 and the variation is shown graphically in figure 6.17.

Similar results are obtained when the second natural frequencies are calculated. The second natural frequency is minimum for orientation angles 0 degrees and 90 degrees and is maximum for orientation angle 45 degrees. The same conclusion can be drawn from these results also. The table 6.11 gives the second natural frequencies for different orientation angles and the figure 6.18 shows the variation graphically.

Sl No.	Orientation angle (deg)	Natural Frequency (Hz)
1	0	15.8601
2	15	16.6982
3	30	19.4021
4	45	21.5245
5	60	19.2045
6	75	16.6124
7	90	15.8286

Table 6.11: Second natural frequencies for a cantilevered plate for different orientation angles

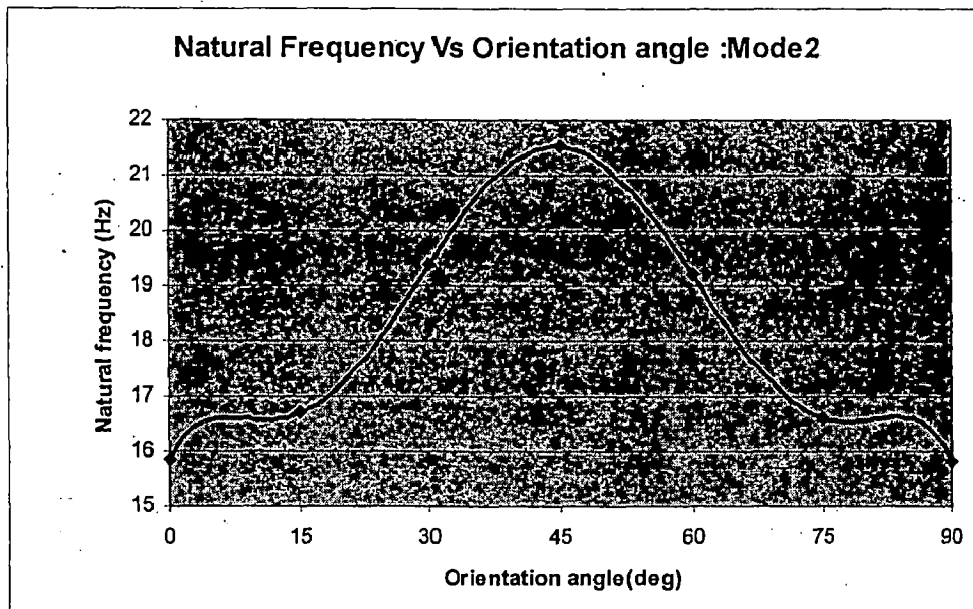


Figure 6.18: The variation of second natural frequency with orientation angle for a cantilevered orthotropic plate

6.3.4. Variation of the fundamental natural frequencies with patch coverage area:

In this problem, the piezoelectric patches are placed over the surface and the variation of the natural frequency is studied. First the piezoelectric patch is covered all over the plate and then the coverage area is gradually reduced to observe the changes in the natural frequency of the plate. The material properties and geometric properties of the plate are taken from the above problem and the piezoelectric material (PZT) are given below.

PZT Patch
 $E_p=6.31 \times 10^7 \text{ N/m}^2$
 $\nu=0.3$
 Density 7760 kg/m^3

Mode No.	Natural Frequency of bare plate	Natural frequency of plate with the patch coverage									
		100%		50%		25%		12%		4%	
		Natural Frequency	%diff	Natural Frequency	%diff	Natural Frequency	%diff	Natural Frequency	%diff	Natural Frequency	%diff
1	14.2926	13.6422	4.55	13.7295	3.94	13.7409	3.86	14.0753	1.52	14.1211	1.20
2	15.8610	14.9823	5.54	15.0505	5.11	15.1821	4.28	15.2821	3.65	15.6865	1.10
3	60.3229	57.4997	4.68	57.7712	4.23	57.9039	4.01	59.7739	.91	59.9609	0.60
4	72.4961	67.5156	6.87	67.6098	6.74	68.4798	5.54	70.8142	2.32	72.3511	0.20
5	72.9922	65.5074	9.64	67.0154	7.56	67.3996	7.03	70.4156	2.87	71.9596	0.74

Table 6.12: Natural frequencies for a cantilevered plate for different coverage area of the piezoelectric patch

However the results obtained do not recommend the optimum coverage area of the patch over the plate, but these results can be used as guidelines for selecting the patch coverage area depending upon the application and the natural frequencies of the system.

The table 6.12 gives the natural frequencies for the bare plate and plate with piezoelectric patch over it. The readings were taken for coverage area 5%, 12%, 25%, 50% and 100% of the plate. As expected, it was observed that the natural frequency is maximum for the bare plate and as we go on covering the plate with the patch the natural frequency goes on decreasing. The decrease in natural frequency is minimum for 5% coverage area and it is maximum for coverage area 100% i.e. patch all over the plate. This reduction in natural frequency is due to the increase in the mass. The stiffness has less effect compared to the effect of increase in mass. The figure shows this reduction graphically for the first five modes.

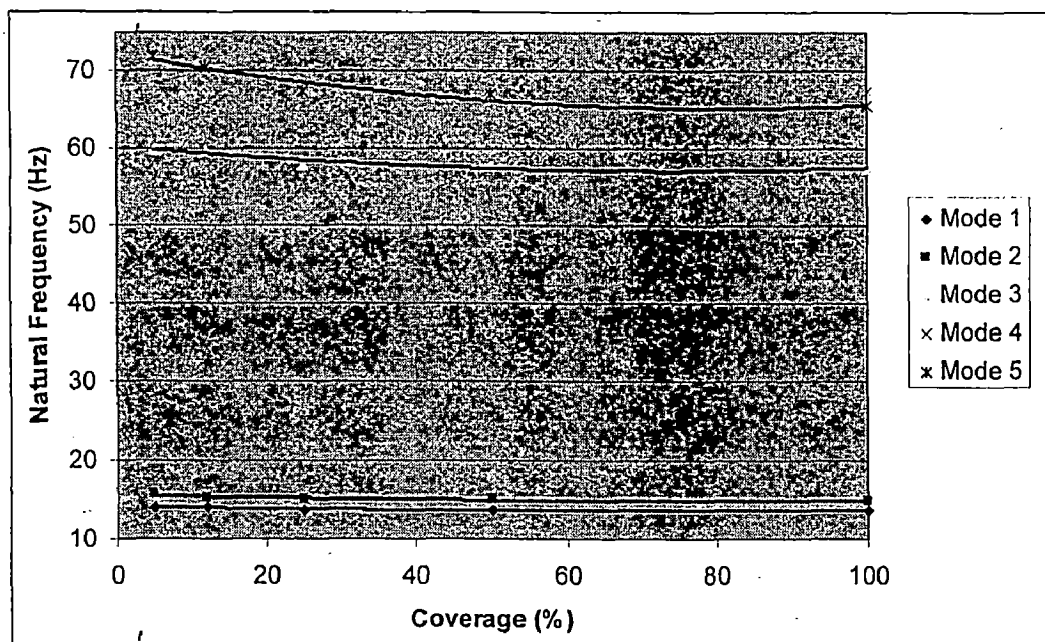


Figure 6.19: The variation of natural frequency with piezoelectric patch coverage area for a cantilevered orthotropic plate.

6.4 Actuator placement optimization:

For the actuator placement problem a $1m \times 1m$ plate is considered. The properties of the plate are taken as in the above problem. The optimization procedure is explained as below.

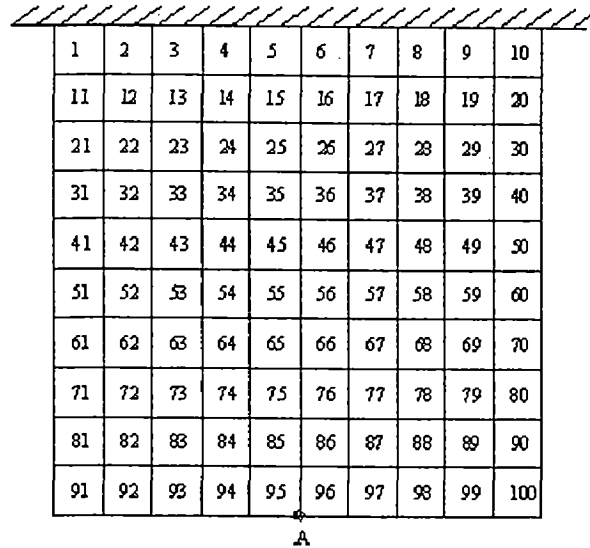


Figure 6.20 Plate surface showing 100 elements

Divide the plate surface into 100 areas with size of $10cm \times 10cm$ as shown in figure 6.20. Four areas will be chosen for bonding piezoelectric patches. To optimize the selection of actuator location, a piezoelectric patch is bonded (imaginarily) on these 100 locations one by one, and in each case an investigation is made to determine the capability of bonded actuator in controlling the vibrations.

6.4.1 Optimization implementation using genetic algorithm

Number the 100 candidate locations from 0 to 99. A chromosome is coded with 32 binary numbers, with each 8 consecutive bits corresponding to an actuator location number from the first bit. With every individual generated by Genetic Algorithm, decode and calculate the corresponding performance index until best individuals are found.

First two modes of the plate are considered. Genetic Algorithm parameters are set as: The number of individuals in a population is 50; Maximal number of

generation is 500; Generation gap is 0.8, which means 40 new individuals are created in the population; Selection function is stochastic universal sampling; Crossover function is single-point crossover; Mutation function is discrete mutation Operator. Normally, genetic algorithm suggests some best solutions only, instead of give the final decision directly. The final decision is still the designer's work. Here, the genetic algorithm optimization is performed for 10 times and the best 12 individuals are listed in Table 6.13.

Actuator Locations	Performance Index values ($\times 10^{-8}$)
1 6 10 84	1.212
2 8 10 94	1.220
1 10 54 84	1.605
1 8 10 38	1.165
1 6 10 57	1.197
1 6 10 84	1.174
1 10 57 84	1.196
1 10 54 57	1.702
1 8 10 94	1.532
1 7 10 84	1.348
1 7 10 67	1.594
1 7 10 57	1.601

Table 6.13: The best 12 individuals obtained by GA.

The final optimized actuator locations

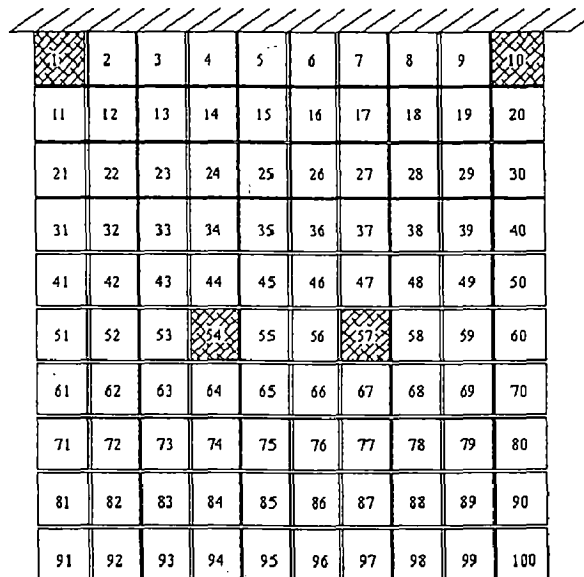


Figure 6.21: Optimized location of actuators over the cantilevered plate.

The problem was also solved considering only the first and second modes to be controlled. The genetic algorithm program is run again to calculate the performance indices and optimal location of actuators over the surface of the plate. The following figures show the location of actuators if only the first and second modes are considered for locating the actuators.

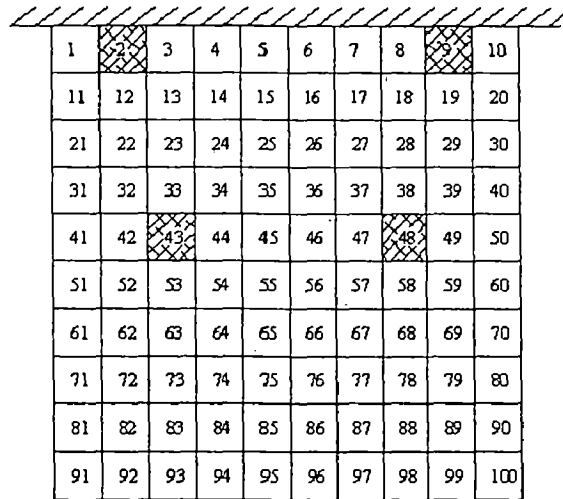


Figure 6.22: Actuator locations when only the first mode is considered

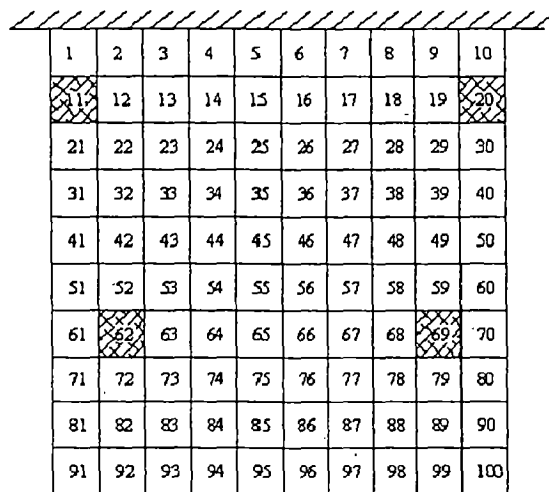


Figure 6.23: Actuator locations when only the second mode is considered

6.5 Time response:

The time response of the system can be obtained by carrying out the modal analysis. In this problem first the time response of the system for free vibration is obtained. The point considered is the point A in the figure: 6.20. Then the force constraints are applied on the system and the system behavior is studied. The

following figure shows the response of the system before and after the application of the forces.

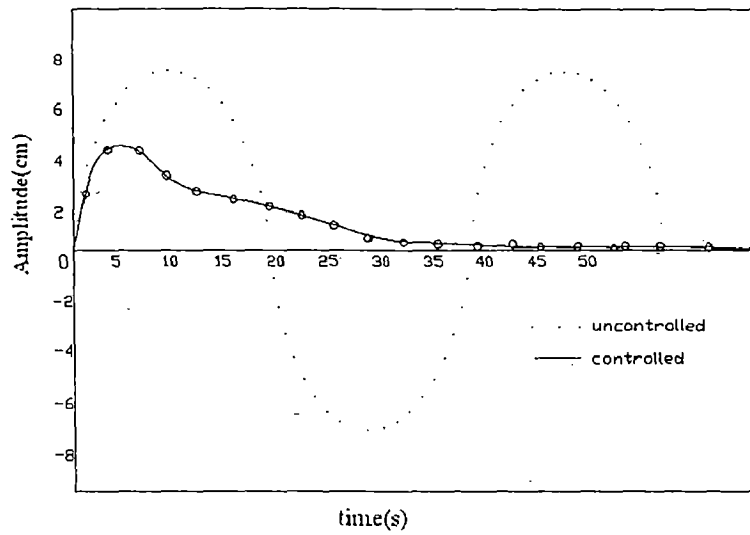


Figure 6.24: Time response of the point A (figure6.20)on the plate before and after the application of force for model

Chapter 7. CONCLUSION

7.1 Conclusion

Smart material and structures have great potential advantages in wide range of applications, such as aeronautical and aerospace engineering etc. In the field of structural shape and vibration control, piezoelectric materials received the most attention because of its low mass, high bandwidth, low cost, etc. This paper develops a method for piezoelectric patches placement optimization. It is based on finite element modeling based on the first order shear deformation theory using MATLAB and controllability grammian maximization and genetic algorithm implementation. The energy dissipation method has been adopted for vibration suppression of the structure. First the static and free vibration analysis is carried to study the variation of static deflection and natural frequencies with the thickness, orientation angle of the fibers of the composite plate, and the patch coverage area over the plate. Computer simulations are performed on optimizing the location of actuators on a rectangular plate. The simulations showed that using this optimization of geometric distribution of piezoelectric patches, the vibration of the structure can be effectively suppressed.

7.2 Scope of future work:

In the current work the dynamic analysis of a cantilever plate is considered and the equations are derived under the assumptions of first order shear deformation theory. The genetic algorithms are used to optimize the location of actuators and the problem shown is the control of a freely vibrating plate. As the future work the reader may consider the plate with different boundary conditions. The work can be extended to control the vibration of a plate under the forced vibration. Further design of the controller circuit will also be a good work that can be done in this field.

REFERENCES

1. Bambill, D. V., Gutierrez, R. H., Laura, P. A. A., and Jederlinic V., 1997, "Vibrations of Composite, doubly connected square membranes," *Journal of Sound and Vibration*, Vol. 203, No. 3, pp. 542-545.
2. Banks, H. T., Smith, R. C., and Wang, Y., 1995, "The Modeling of Piezoceramic Patch Interactions with Shells, Plates, and Beams," *Quarterly of Applied Mathematics*, Vol. LIII, No. 2, pp. 353-381.
3. Clayton L. Smith, 2001, *Analytical Modeling and Equivalent Electromechanical Loading Techniques for Adaptive Laminated Piezoelectric Structures*", Ph.d. thesis, Virginia Polytechnic Institute and State University, Blacksburg, Virginia
4. Crawley, E.F., and de Luis, J., 1987 "Use of Piezoelectric Actuators as Elements of Intelligent Structures," *AIAA Journal*, Vol. 25, No. 10, pp. 1373-1385
5. Collins, S. A., Miller, D. W., and von Flotow, A. H., 1990 "Sensors for Structural Control Applications using Piezoelectric Polymer Film," *Masters Thesis*, Massachusetts Institute of Technology.
6. Cox, D. E. and Linder, D. K., 1991, "Active Control for Vibration Suppression in a Flexible Beam using a Modal Domain Optical Fiber Sensor", *Journal of Vibration and Acoustics*, Vol.113, 369-382.
7. Garcia Sandrine, 1999, "Experimental design optimization and Thermophysical parameter estimation of composite materials Using genetic algorithms.", *Masters Thesis* submitted to Virginia Polytechnic Institute and State University, UNIVERSITE DE NANTES ISITEM, Nantes, France

8. Hagood, N. W., Chung, W. H. and von Flotow, A., 1990, "Modelling of Piezoelectric Actuator Dynamics for Active Structural Control," Proceedings, 31st AIAA/ASME/ASCE/AHS Structures, Structural Dynamics and Materials Conference, Long Beach, CA, pp. 2242-2256.
9. Hinton E.M., Ozakca and N. V. R. Rao, 1995, "Free vibration analysis and shape Optimization of variable thickness Plates, prismatic folded plates and Curved shells, part 1: finite strip Formulation, Journal of Sound and Vibration , 181(4), pp. 442-455
10. Jinsong, Asundi, A. and Liu, Y., 1998, "Vibration Control of Smart Composite Beams with Embedded Optical Fiber Sensor and ER Fluid", JVA-98-072, pp. 1-4.
11. Jha A. K., 2002, "Vibration analysis and control of an inflatable toroidal satellite component using piezoelectric actuators and sensors", Ph.d. thesis, Virginia Polytechnic Institute and State University, Blacksburg, Virginia
12. Kulkarni, G. and Hanagud, S. V., 1991, "Modeling Issues in the Vibration Control with Piezoceramic Actuators," Transactions of the ASME: Smart Structures and Materials AD-Vol.24/AMD-Vol. 123, pp. 253-268
13. Langley, R. S., 1995, "The Effect of Attachments on the Natural Frequencies of a Membrane," Journal of Sound and Vibration, Vol. 188, No. 5, pp. 760-766.
14. Liew K.M., J. Z. Zhang, T. Y. Ng, J. N. Reddy, 11/2003, Dynamic Characteristics of Elastic Bonding in Composite Laminates: A Free Vibration Study", Transactions of the ASME,, Vol. 70, pp. 860-870
15. Makhecha D.P., Ganapathi M. and b. P. Patel B.P., 2002, "Vibration and damping analysis of laminated/sandwich composite plates using Higher-Order Theory", Journal of reinforced plastics and composites, Vol. 21, pp. 559-575.
16. Masad, J. A., 1996,, "Free Vibrations of a Non-Homogeneous Rectangular Membrane," Journal of Sound and Vibration, Vol. 195, No. 4, pp. 674-678.

17. Payman Afshari and G. E. O. Widera, 08/2000, "Free Vibration Analysis Of Composite Plates, Transactions of the ASME, Vol. 122, pp. 390-398
18. Peng F., Ng Alfred and Ru Hu Yan, 2003, "Adaptive vibration control of flexible structures with actuator placement optimization", Proceedings of IMECE'03, 2003 ASME International Mechanical Engg Congress, Washington, IMECE2003, pp 1-10
19. Pronsato, M. E., Laura, P. A. A. and Juan, A., 1999, "Transverse Vibrations of a Rectangular Membrane With Discontinuously Varying Density," Journal of Sound and Vibration, Vol. 222, No. 2, pp. 341-344.
20. Rajeev kumar, Ashish Srivastav, B.K. Mishra and S.C.Jain, 2003, "Finite element formulation and active vibration control using real coded genetic algorithm", Proceedings of the International Conference on Mechanical Engineering 2003, ICME2003-ABS-03/106, Dhaka, Bangladesh.
21. Reddy, J.N. "Mechanics of Laminated Composite Plates". CRC Press, 1997.
22. Reddy. J.N, 1998, "Theory and analysis of elastic plates", Taylor and Francis US.
23. Reddy J.N., 2003, "An introduction to the finite element method", Tata McGraw-Hill publishing company limited, New Delhi.
24. Saravanos, Dimitris A., 1997, "Mixed Laminate Theory and Finite Element for Smart Piezoelectric Composite Shell Structures". AIAA Journal, Vol. 35, No. 8, pp. 511-525
25. Shimpi R.P. and V. Ainapure, 4/2004, "Free vibration of two-layered cross-ply laminated plates", Journal of reinforced plastics and composites, vol. 23, no., 389-405.
26. Suleman, A. And Venkayya, V.B., 11/1995, "A Simple Finite Element Formulation for a Laminated Composite Plate with Piezoelectric Layers", Journal of Intelligent Material Systems and Structures, Vol 6, pp. 522-568

27. Sze, K. Y. and Yao, L. Q., 2000, "Modeling Smart Structures with Segmented Piezoelectric Sensors and Actuators", *Journal of Sound and Vibration*, Vol.235(3), pp. 495-520.
28. Van Niekerk, J. L. and Tongue, B. H., 1995, "Active Control of a Circular Membrane to Reduce Transient Noise Transmission," *Journal of Vibration and Acoustics*, Vol. 117, No. 7, pp. 252-258.
29. Wang, B. T., and Chen, R. L., 2000, "The Use of Piezoceramic Transducers for Smart Structural Testing," *Journal of Smart Material Systems and Structures*, Vol. 11, September, pp. 1-12.
30. Yan Y,J, and Yam L.H., 2002, "Optimal design of number and locations of actuators in active vibration control of a space truss.", *smart materials and structures*, vol. 11, pp 496-503